Modelling dryland winter wheat yield using remotely sensed imagery and agrometeorological parameters

by

Zinhle Olga Mashaba

Submitted in partial fulfilment of the requirements

for the degree of

MASTER OF SCIENCE

GEOINFORMATICS

in the

Faculty of Natural and Agricultural Science

University of Pretoria

2016

Declaration of originality

This is to declare that the research work presented here is entirely my own work, unless or otherwise explicitly acknowledged by citation of published and unpublished sources. This research has not previously been submitted for assessment in any form to the University of Pretoria or to any other institution for any other purposes.

Signature: Date:

Modelling dryland winter wheat yield using remotely sensed imagery and agrometeorological parameters

Author Zinhle Olga Mashaba
Supervisors [1,4]Dr. Joel Botai
[2]Dr. George Chirima
[3,4]Prof. Ludwig Combrinck
Affiliations [1]South African Weather Services, Pretoria, South Africa
[2]Geoinformatics Division, Agricultural Research Council, Pretoria, South Africa
[3]Hartebeesthoek Radio Astronomy Observatory, Krugersdorp, South Africa
[4]Department of Geography, Geoinformatics and Meteorology University of Pretoria, Pretoria, South Africa
Degree Master of Science Geoinformatics

Abstract

Wheat consumption has become more widespread and is increasing in South Africa especially in the urban areas. The wheat industry contributes four billion rands to the gross value of agriculture and is a source of employment to approximately 28 000 people. Wheat yield forecasting is crucial in planning for imports and exports depending on the expected yields and wheat health monitoring is important in minimizing crop losses. However, current crop surveying techniques used in South Africa rely on manual field surveys and aerial surveys, which are costly and not timely (after harvest). This research focuses on wheat health monitoring and wheat yield prediction using remote sensing, which is a cost effective, reliable and time saving alternative to manual surveys. Hence, the research objectives were: (i) to identify remotely sensed spectral indices that comprehensively describe wheat health status. (ii) Develop an Normalized Difference Vegetation Index (NDVI) based wheat yield forecasting model and (iii) to evaluate the impact of selected agrometeorological parameters on the NDVI based forecasting model. Landsat 8 images were used for determining spectral indices suitable for wheat health monitoring by relating the spectral indices to the land surface temperature. Results show that the Normalized Difference Water Index (R^2 between 0.65 and 0.89) and NDVI (R^2 between 0.36 and 0.62) were the most suitable indices for wheat health status monitoring. Whereas, the

Normalized Difference Moisture Index (R^2 between 0.53 and 0.79) and the Green Normalized Difference Vegetation Index (R^2 between 0.28 and 0.41) were found to be less suitable for wheat health monitoring. Moderate Resolution Spectroradiometer (MODIS) derived NDVI for fourteen years was used to build and test a wheat yield forecasting model. The model was significant with an R^2 value of 0.73, a p-value of 0.00161 and an RMSE of 0.41 tons ha^{-1}. The study established that the period 30 days before harvest during the anthesis growth stage, is the best period to use the linear regression model for wheat yield forecasting. Satellite derived agrometeorological parameters such as: soil moisture, evapotranspiration and land surface temperature were added to the NDVI based model to form a multi-linear regression model. The addition of these parameters to the NDVI model improved it from an R^2 of 0.73 to an R^2 of 0.82. Through the use of a correlation matrix, the NDVI (r=0.88) and evapotranspiration (r=0.58) were highly correlated to wheat yield as compared to soil moisture (r=0.27) and land surface temperature (r=-0.02). This research provided evidence that remote sensing can be used at acceptable levels of accuracy for wheat monitoring and wheat yield predictions compared to manual field surveys which are costly and time consuming.

Keywords: remote sensing, wheat yield, forecasting, monitoring, spectral indices

Acknowledgements

I would like to acknowledge the following:

Dr G. Chirima: for his support, critical comments and motivation. Through his leadership, my research skills have improved.

Dr J. Botai: for his guidance and encouraging me to further my studies.

Prof L. Combrinck: for his critical comments and advice on language usage, which was very useful.

Institutions: the Agricultural Research Council-Institute for Soil Climate and Water (ARC-ISCW), ARC-Small Grain Institute, GeoTerra Images (GTI), Spatial Business IQ (SIQ) are acknowledged for the data used in this research and the Centre for Geoinformation Science at the University of Pretoria for their continued support.

Funding: the ARC Professional Development Programme, GTI, SIQ, National Research Foundation and the University of Pretoria are acknowledged for funding this research.

Family: my father Mr Jude Mashaba and mother Ms Dorothy Mashaba for their love and investing time in nurturing my academic development from a young age. My two sisters Wandile and Lungile Mashaba are acknowledged for their upliftment during this research. I am also thankful to my fiancé Cilence Munghemezulu for his unconditional love, patience and encouragement.

Colleagues: Mr Philemon Tsele is acknowledged for his encouragement. I would also like to thank my colleagues at ARC: Sithembele, Kgaogelo, Reneilwe, Siphokhazi and Tshepiso for creating a warm environment at work.

Publications and Proceedings

Peer-reviewed:

1. Mashaba, Z., Chirima, G., Botai, J., Combrinck, L. and Munghemezulu, C., 2016. Evaluating spectral indices for winter wheat health status monitoring in Bloemfontein using Landsat 8 data. *South African Journal of Geomatics*. 5(2), 227-243, http://dx.doi.org/10.4314/sajg.v5i2.10.

2. Mashaba, Z., Chirima, G., Botai, J., Combrinck, L., Munghemezulu, C. and Dube, E., 2016. Forecasting winter wheat yields using MODIS NDVI data for the Central Free State Region. *South African Journal of Science*. (Accepted, manuscript ID: SAJS-2016-0201.R2).

3. Mashaba, Z., Chirima, G., Botai, J. and Munghemezulu, C., 2017. Evaluating the influence of agrometeorological parameters for winter wheat yield forecasting. *South African Geographical Journal*. (Submitted, manuscript ID: RSAG-2017-0021).

Conferences:

1. Mashaba, Z., Chirima, G., Botai, J. and Combrinck, L., 2015. The potential of analysing wheat yield parameters by integrating remotely sensed imagery and crop simulation models. Agricultural Research Council Professional Development Programme Conference. Hatfield South Africa. 26-28 October 2015.

2. Mashaba, Z., Chirima, G., Botai, J. and Combrinck, L., 2016. Investigating the influence of temperature variability on wheat in Bloemfontein using Landsat 8 data. International Crop Modelling Symposium (iCropM2016). Berlin Germany. 15-17 March 2016.

3. Mashaba, Z., Chirima, G., Botai, J. and Combrinck, L., 2016. Evaluating spectral indices for winter wheat health status monitoring in Bloemfontein using Landsat 8 data. Geomatics Indaba. Kempton Park South Africa. 12-14 September 2016.

4. Mashaba, Z., Chirima, G., Botai, J. and Combrinck, L., 2016. Forecasting dryland winter wheat yields using MODIS NDVI data. Agricultural Research Council Professional Development Programme Conference. Roodeplaat South Africa. 24-25 October 2016.

Table of Contents

List of Figures

List of Tables

List of Abbreviations

AMSR	Advanced Microwave Scanning Radiometer
AVHRR	Advanced Very High Resolution Radiometer
BRDF	Bidirectional Reflectance Distribution Function
CMI	Crop Moisture Index
CV-MVC	Constrained view maximum value composite
ET	Evapotranspiration
ETM+	Landsat Enhanced Thematic Mapper plus
EVI	Enhanced Vegetation Index
FLAASH	Fast Line-Of-Sight Atmospheric Analysis Of Spectral Hypercubes
GLDAS	Global Land Data Assimilation System
GNDVI	Green Normalized Difference Vegetation Index
GNSS	Global Navigation Satellite Systems
IDL	Interactive Digital Language
LAI	Leaf Area Index
LST	Land Surface Temperature
MBE	Mean Bias Error
MODIS	Moderate Resolution Imaging Spectroradiometer
MRT	Modis Reprojection Tool
MSS	Multispectral Scanner
NASA-EOS	National Aeronautical Space Agency-Earth Observing System
NDMI	Normalized Difference Moisture Index
NDVI	Normalized Difference Vegetation Index
NDWI	Normalized Difference Water Index
NIR	Near Infrared
NOAA	National Oceanic And Atmospheric Administration
PWV	Precipitable Water Vapour
Q-Q	Quantile-Quantile
RE	Relative Error
RMSE	Root Mean Square Error
SAR	Synthetic Aperture Radar
SE	Standard Error

S-G	Savitzky-Golay
SM	Soil Moisture
SMI	Soil Moisture Index
SPOT	Système Pour l'Observation De La Terre
TCI	Temperature Condition Index
TDVI	Temperature Dryness Vegetation Index
TOA	Top of Atmosphere
UAV	Unmanned Aerial Vehicle
USGS	United States Geological Survey
VCI	Vegetation Condition Index

Chapter 1
General Introduction

1.1. Introduction

South Africa is a producer of different crops such as maize, wheat, sorghum, canola, barley, groundnuts, sunflower seeds, sweet lupines, soybeans and dry beans (DA, 2006). The wheat industry contributes four billion rands to the gross value of agriculture and is a source of employment to approximately 28 000 people (DAFF, 2012). The provinces, which produce large quantities of wheat within South Africa, are the Western Cape, Northern Cape and Free State (DAFF and Agbiz, 2014). The wheat produced in South Africa is mainly used for human consumption (bread, rusks, biscuits etc.) and a smaller proportion is used for the production of pasta. Additionally, low quality wheat is used as seeds, feed stock and has other industrial uses (DAFF, 2006).

Current methods for wheat monitoring and yield estimations are reliant on ground based surveys and aerial surveys, which are time consuming and expensive. In addition to these techniques, field interviews are also conducted with farmers who are often reluctant to give information on their crop yields; the estimates given by farmers are sometimes inaccurate. Using these manual techniques provides wheat yield estimates after harvest, which affects the planning of imports and exports. The use of low cost Unmanned Aerial Vehicles (UAVs) can overcome these limitations and have an improved accuracy as compared to low resolution satellite imagery on a farm scale or field trails. However, these techniques are not suitable for regional crop yield forecasting (Grenzdörffer et al., 2008; Berni et al., 2009). In addition to these challenges, climate variability in most summer rainfall areas has decreased soil moisture, which has affected the yield of dryland crops. This has led to a significant number of farmers converting to sustainable crops due to the low productivity of wheat (Breitenbach and Fényes, 2000).

Satellite remote sensing can be used in agricultural applications because it is cost effective, reliable and time saving (Sethi et al., 2014). Through the use of remotely sensed imagery, wheat monitoring and wheat yield forecasting can be done prior to

harvest as compared to manual surveys of yields. Hence, this research focused on developing satellite remote sensing based methods for modelling dryland wheat yields in terms of wheat health status monitoring and wheat yield forecasting.

1.1.1. Remote Sensing for crop yield estimation

Agricultural applications that rely on remotely sensed data are based on the assumption that spectral data are related to canopy reflectance parameters, which in turn, are related to the final yields (Singh et al., 2002; Ferencz et al., 2004). Different indices such as the normalized difference vegetation index (NDVI), vegetation condition index (VCI) and the temperature condition index (TCI) are derived from remote sensing imagery to determine the health status of certain crops (Kogan, 2001; Kogan, 2002; Singh et al., 2003). The NDVI values range between 1 and -1 where values close to 1 represent healthy dense vegetation and values close to -1 represent unhealthy vegetation (Singh et al., 2003). The VCI and TCI are dimensionless indices, derived using the NDVI and brightness temperature. When these two indices are greater than 70, then vegetation is healthy and conversely, an opposite trend is observed when vegetation is stressed (Kogan, 2001; Kogan, 2002).

Numerous studies have used remotely sensed satellite imagery for crop yield estimations. Labus et al., (2002) demonstrated that multi-temporal NDVI satellite imagery can be used for wheat yield estimates in Montana, United States of America. In that study, it was established that Advanced Very High Resolution Radiometer (AVHRR)-NDVI biweekly satellite imagery provides accurate wheat yield estimates at a regional scale but has uncertainties at a farm level. Shao et al., (2001) developed a method to monitor rice growth for production estimation utilizing multi-temporal Radarsat data in China. In that study, it was established that classifying multi-temporal Radarsat imagery has an accuracy of 91% in mapping rice. Jackson et al., (2004) demonstrated that Landsat derived Normalized Difference Water Index (NDWI) can be used for yield estimation and also compared its accuracy with the NDVI for maize and soybeans. In the study, the NDWI proved to be superior as compared to the NDVI derived from Landsat data. Prasad et al., (2006) developed a crop prediction model using different kinds of remote sensing data such as AVHRR, National Oceanic and

Atmospheric Administration (NOAA), Système Pour l'Observation de la Terre (SPOT) and Landsat Multispectral Scanner (MSS) for maize and soybean yield in Iowa USA.

Crops such as maize, wheat, soybean and rice form part of the staple diet of South Africans. However, few studies have been done on using remote sensing data for yield estimation in South Africa. For example, Unganai and Kogan (1998) demonstrated that maize yields can be estimated using AVHRR data. In the study, it was found that VCI and TCI derived from AVHRR data are highly correlated with maize yield. Frost et al., (2013) demonstrated that the Terra Moderate Resolution Imaging Spectroradiometer (MODIS) satellite sensor data products can be applied for maize yield estimation in South Africa. In that study, the window method was utilized and the resulting window periods proved that average NDVI and average Enhanced Vegetation Index (EVI) data can be used for maize yield estimations. There is a need for more studies to be done in South Africa on using remote sensing for yield predictions. This need arises as current crop yield estimates rely on manual field surveys that are done at the end of the growing season, which is not timely for wheat management. During field interviews, farmers are reluctant to give exact yield estimates for their crops.

1.1.2. Remote Sensing for crop health monitoring

Crop health status monitoring is crucial for food security. Through the knowledge of the current crop growing conditions, improvements can be made during the season to maximize crop yields. For example, water shortages can be determined early in the season using remote sensing technologies and the irrigation patterns can be altered for better yields at harvest. The commonly used remote sensing based methods for crop monitoring are classification methods and crop models. Classification methods use remotely sensed satellite images to classify farmland into different classes (Ji-hua and Bing-fang, 2008). Principally, supervised and unsupervised classification methods have been reliable for this purpose (Abuzar et al., 2000; Kuenzer and Knauer, 2013). These approaches can be used for the identification of farms, which have healthy or unhealthy crops. The main challenge of the mentioned methods is discriminating

between pixels (i.e. an ambiguity exists), which correspond to a certain crop type when there are mixed land uses (Löw and Duveiller, 2014).

Crop growth models are used to simulate the biophysical processes, which take place in the soil, crop and atmosphere to understand the growth and development of a crop (Doraiswamy et al., 2003). Crop growth models are commonly linked with remotely sensed data for crop monitoring applications (Moulin et al., 1998). The limitations of crop growth models are that they are less accurate when applied in non-optimal growing conditions. This limitation can be overcome by coupling crop growth models with remotely sensed data (i.e. Leaf Area Index (LAI)) to represent the actual growing conditions (Clevers and van Leeuven, 1996). Crop models often require input data that might not be available for a particular site for example, solar radiation (Hoogenboom, 2000).

1.1.3. General study area description

The Free State province (Figure 1) covers an area of approximately 129 825 km² in South Africa. The province is intersected by the Vaal River in the north and the Orange River in the south. Towards the South East, the Free State shares an international border with Lesotho. Within the province, there are five-district municipalities-Thabo Mofutsanyana, Mangaung, Xhariep, Lejweleputswa and Fezile Dabi (DRDLR, 2009; DRDLR, 2013). The Thabo Mofutsanyana district consists of hills and fruit farms. The Mangaung district is the main trade and administrative centre. The Xhariep district consists of farmlands and dispersed towns; it is mostly covered by grassland. The Lejweleputswa district is important for the Gross Domestic Product (GDP) of South Africa as the district hosts gold mining industries and maize production areas. The Fezile Dabi district is an important agricultural producer of maize (FSP, 2005).

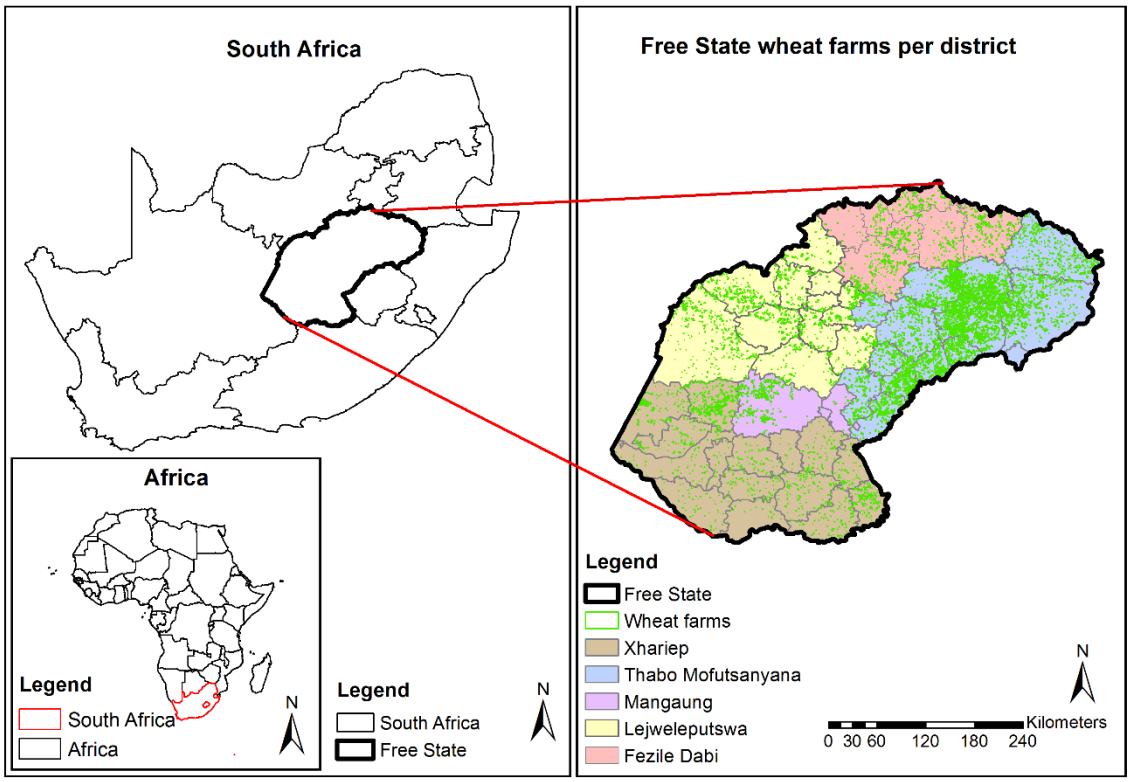

Figure 1. Location of the Free State study area and the wheat production farms within each municipal district.

The temperatures of the Free State are low in winter (minimum of -5 °C) and high (maximum of 35 °C) in summer. The eastern areas experience low temperatures and infrequent light snowfall due to the high mountain ranges, whereas, the western areas experience high temperatures. The rainy season occurs during the summer months, from September to March. The annual average rainfall is between 600 mm and 750 mm in the east and less than 300 mm in the west. There is an occurrence of frost from May to September in the west although the frost can extend to October in the East (DRDLR, 2013).

The soils of the Free State have a soil depth ranging from 600 mm to 900 mm in the eastern, western and northern parts of the province. Deeper soils are found in the Northern and Western Free State, which contribute to its higher crop yield. The topography is suitable for agriculture. The eastern and north eastern areas are high lying while the eastern and southern borders are mountainous (NDA, 2002).

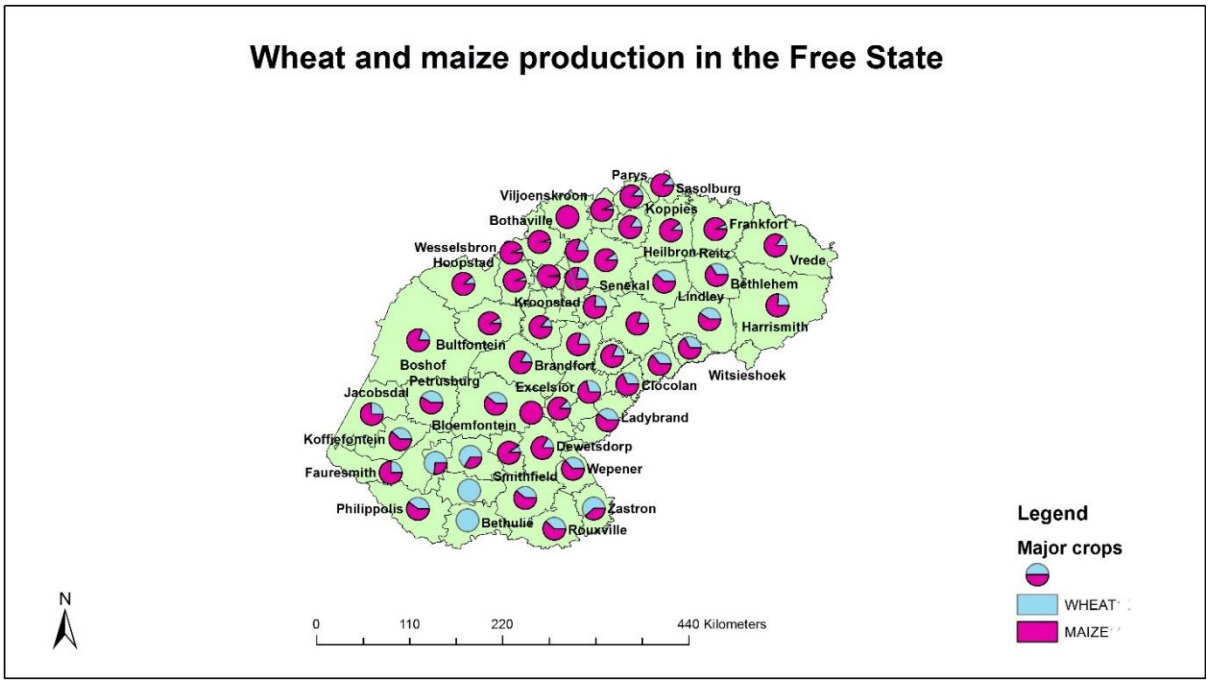

Figure 2. The relative distribution of maize and wheat in the Free State.

Agricultural activity in the Free State is divided between mixed livestock and crop farming. The cultivated land covers approximately 3.2 million hectares and the grazing land covers approximately 8.7 million hectares of land (NDA, 2002). In terms of crop production, the Free State contributes 41% of the maize in South Africa and 30% of the wheat in South Africa (NDA, 2005; SAGL, 2013). In Figure 2, the wheat production areas of Free State are depicted relative to the maize production areas. The Thabo Mofutsanyana district is one of the largest wheat producers. The other food crops grown in the province are sorghum, canola, barley, groundnuts, sunflower seeds, sweet lupines, soybeans and dry beans (DA, 2006). The crops produced are mostly rain-fed and only a small portion of approximately 10% is irrigated (Moeletsi and Walker, 2012).

1.2. Problem statement

The use of remote sensing technologies has allowed many scientists to manage environmental challenges due to its non-invasiveness and ability to give a synoptic view of features on ground targets (Lamb and Brown, 2001). In agricultural applications, there is a need for crop yield estimation and crop health monitoring. In South Africa, crop yield estimation methods rely on field visits, interviewing farmers and aerial surveys of crops. These methods are time consuming, costly, inconsistent and labour intensive and the information collected is not timely for decision-making. However, the use of low cost UAVs can overcome the challenges of timeliness and consistency on a farm scale or field trails, but not on a regional scale (Grenzdörffer et al., 2008; Berni et al., 2009).

The use of satellite remotely sensed imagery provides a timely, cost effective and reliable alternative to traditional methods for surveying crop yield. However, there are limited studies on remote sensing based crop yield forecasting in South Africa. Most studies are done on small areas and do not integrate agrometeorological parameters in the yield models for example Unganai and Kogan, (1998) and Frost et al., (2013). Meanwhile, the addition of agrometeorological parameters in crop yield forecasting models incorporates information about the environmental conditions, which influence crop growth. These factors have made it necessary to use satellite remote sensing technology to predict crop yield on large areas.

Crop health monitoring is another important process during the physiological growth of a crop. The use of remote sensing for crop health monitoring is not well explored in South Africa. Knowledge of the health status of crops can help farmers to apply mitigation methods to prevent or decrease crop losses earlier on in the season by adding fertilizers, applying herbicides or changing irrigation methods. Remote sensing can be used for both crop yield estimation and crop health monitoring. Additional applications of remote sensing in agriculture are in estimating crop parameters such as biomass, potential evapotranspiration, and surface soil moisture (Bastiaanssen et al., 2000).

1.3. Aim and objectives

The aim of the study was to assess the application of remotely sensed spectral indices derived from MODIS, and Landsat 8 and, agrometeorological parameters to monitor dryland winter wheat health and forecast yields in the Free State Province. The following specific objectives provided guidance to achieve the overarching research goal:

1. To identify remotely sensed spectral indices that comprehensively describe wheat health status.
2. To develop a Normalized Difference Vegetation Index (NDVI) based wheat yield forecasting model.
3. To evaluate the impact of agrometeorological parameters on the NDVI based wheat yield forecasting model.

1.4. Significance of the research

This research aids in understanding the historic and current trends in wheat yield by integrating remotely sensed satellite imagery and agrometeorological parameters. This application is of particular importance as large amounts of wheat are currently being imported into South Africa as the current domestic production of wheat only meets 55% of the national demand (DAFF and Agbiz, 2014). Crop forecasting allows decision makers in various sectors to plan for exports if there is an excess amount of wheat and imports if there is a shortage of wheat. However, manual field surveys for crop yield estimations are done at the end of the growing season and are expensive. Remote sensing provides a cost effective and non-obtrusive method of forecasting crop yields during the growing season.

This research is also significant in terms of food security, which is defined as the availability of food that is nutritious and safe, acquired in a socially acceptable way (Labadarios et al*.,* 2011). With the application of remote sensing techniques, accurate estimates of wheat yields and an indication of wheat health status can be obtained before harvest to determine wheat availability, thereby, improving food security.

With the increasing human population in South Africa, agricultural land is becoming limited and built up areas are increasing. This puts pressure on the current agricultural land to produce more food. Whereas, more farmers are converting from wheat farming to profitable crops such as soybeans or maize (Breitenbach and Fényes, 2000), this poses a threat to the current wheat supply. Therefore, it is important to use wheat yield forecasting and monitoring techniques, which are accurate to enhance the current management of wheat.

1.5. Thesis structure

This thesis contains five chapters. The thesis is written in a format such that, each chapter has an abstract, introduction, background, data and methods, result and discussion, conclusion and references section (with exception to Chapter 1 and Chapter 5 which do not have abstracts, methods, results and discussion sections). There is some repetition of information (i.e. references and study area) in the chapters due to this structure. After each introduction section, a literature review is given (with exception to Chapter 5), thus, an independent literature review section is not included in the thesis. This adopted structure aids in categorizing information relating to each of the three objectives together.

Chapter 2: Evaluating spectral indices for winter wheat health status monitoring

In Chapter 2, spectral indices derived from Landsat 8 images were evaluated for the objective of identifying indices, which are closely related to wheat health status. Monitoring wheat health during the growing season is vital for minimizing crop losses and predicting crop yield. This chapter outlines the phenological growth of wheat, fundamentals of remote sensing and methods for crop monitoring. Then, statistical analyses are performed to verify the performance of each of the spectral indices. The results are summarized and discussed to make conclusions. The spectral index related to wheat health status evaluated in this chapter is used in Chapter 3 and Chapter 4 for the development of wheat yield forecasting models.

Chapter 3: Forecasting dryland winter wheat yields using MODIS NDVI data

In this chapter, the second objective of developing a wheat yield forecasting model from MODIS derived NDVI imagery is addressed. Crop yield forecasting is often done at critical stages of crop growth. Hence, this chapter also focuses on investigating whether the anthesis wheat growth stage is suitable for wheat yield forecasting. A review of remote sensing for crop yield prediction and the MODIS vegetation products is provided. The procedure of processing fourteen years of MODIS data and wheat yield data for the generation, validation and testing of a wheat-forecasting model is described. The results are summarized and discussed to make conclusions. The model derived in this chapter was modified in Chapter 4 to evaluate the influence of integrating agrometeorological parameters in the model for wheat yield forecasting.

Chapter 4: Evaluating the influence of agrometeorological parameters for winter wheat yield forecasting

In this chapter, satellite derived agrometeorological parameters are incorporated to the NDVI based model from Chapter 3 to investigate their influence on wheat yield forecasting. The use of agrometeorological parameters in yield models incorporates information on the environmental conditions, which influence crop growth and how they affect the accuracy of the NDVI based model. The background on the two common agrometeorological parameter based methods used for crop forecasting are presented in this chapter. In particular, the parameters important for non-irrigated wheat forecasting comprising the NDVI, soil moisture, evapotranspiration and surface temperature were used for the development of the wheat yield forecasting model. Statistical tests were done to validate and test the calibrated model. The relative importance of each parameter was determined. The results were then summarized and discussed to draw conclusions.

Chapter 5: Conclusion and Recommendations

Chapter 5 deals with an overview of the research findings and links each chapter in the context of wheat yield modelling. The first group of questions concerned the broader issues of assessing and identifying i) which indices were suitable for application in forecasting wheat yields and ii) whether the anthesis growth stage was relevant for use in developing yields models? The second involved assessing the influence of incorporating agrometeorological parameters in wheat yield forecasting models. These are discussed in the context of the three research objectives and recommendations for future research using satellite imagery for crop forecasting and crop monitoring are provided.

1.6. References

1. Abuzar, M., McAllister, A. and Morris, M., 2000. Classification of seasonal images for monitoring irrigated crops in a salinity-affected area of Australia. *International Journal of Remote Sensing*, 22(5), 717-726.
2. Bastiaanssen, W.G., Molden, D.J. and Makin, I.W., 2000. Remote sensing for irrigated agriculture: examples from research and possible applications. *Agricultural Water Management*, 46, 137-155.
3. Berni, J.A.J., Zarco-Tejada, P.J., Suárez, L., González-Dugo, V. and Fereres, E., 2009. Remote sensing of vegetation from UAV platforms using lightweight multispectral and thermal imaging sensors. *International Archives of Photogrammetry Remote Sensing and Spatial Information Science*, 38(6).
4. Breitenbach, M.C. and Fényes, T.I., 2000. Maize and wheat production trends in South Africa in a deregulated environment. *Agrekon*, 39, 292-312.
5. Clevers, J.G.P.W. and Van Leeuwen, H.J.C., 1996. Combined use of optical and microwave remote sensing data for crop growth monitoring. *Remote Sensing of Environment*, 56(1), 42-51.
6. DA, 2006. Crops and Markets. Department of Agriculture. Pretoria.
7. DAFF, 2006. Wheat, DAFF, Gauteng, Pretoria.
8. DAFF, 2012. Wheat market value chain profile, DAFF, Gauteng, Pretoria.
9. DAFF and Agbiz, 2014. JADAFA Agricultural Outlook Brief: South Africa's Commodity Markets. Spear and BFAP. Pretoria.
10. Doraiswamy, P.C., Moulin, S., Cook, P.W. and Stern, A., 2003. Crop Yield Assessment from Remote Sensing. *Photogrammetric Engineering and Remote Sensing*, 69, 665-674.
11. DRDLR, 2009. Free State Comprehensive Rural Development Programme (CRDP). Department of Rural Development and Land Reform. Pretoria.
12. DRDLR, 2013. Free State Province Spatial Development Framework (PSDF). Department of Rural Development and Land Reform. Pretoria.
13. Ferencz, C., Bognar, P., Lichtenberger, J., Hamar, D., Tarcsai, G., Timar, G., Molnar, G., Pasztor, S., Steinbach, P., Szekely, B., Ferencz, O.E. and Ferencz-Arkos, I., 2004. Crop yield estimation by satellite remote sensing. *International Journal of Remote Sensing*, 25, 4113-4149.
14. Frost, C., Thiebaut, N. and Newby, T., 2013. Evaluating Terra MODIS Satellite Sensor Data Products for Maize Yield Estimation in South Africa. *South African Journal of Geomatics*, 2, 106-119.
15. FSP, 2005. Free State Province Provincial Growth and Development Strategy (PGDS) 2005 - 2014. Free State Provincial Government, Bloemfontein.
16. Grenzdörffer, G.J., Engel, A. and Teichert, B., 2008. The photogrammetric potential of low-cost UAVs in forestry and agriculture. *The International Archives of the Photogrammetry, Remote Sensing and Spatial Information Sciences*, 31(B3), 1207-1214.

17. Hoogenboom, G., 2000. Contribution of agrometeorology to the simulation of crop production and its applications. *Agricultural and Forest Meteorology*, 103(1), 137-157.
18. Jackson, T., Chen, D., Cosh, M., Li, F., Anderson, M., Walthall, C., Doriaswamy, P. and Hunt, E.R., 2004. Vegetation water content mapping using Landsat data derived normalized difference water index for corn and soybeans. *Remote Sensing of Environment*, 92, 475-482.
19. Ji-hua, M. and Bing-fang, W., 2008. Study on the crop condition monitoring methods with remote sensing. *International Archives of the Photogrammetry, Remote Sensing and Spatial Information Sciences*, 37(B8), 945-950.
20. Kogan, F.N., 2001. Operational space technology for global vegetation assessment. *Bulletin of the American Meteorological Society,* 82(9), 1949–1964.
21. Kogan, F.N., 2002. World Droughts in the new millennium from AVHRR-based vegetation health indices. *EOS Transactions of the American Geophysical Union*, 48, 562–563.
22. Kuenzer, C. and Knauer, K., 2013. Remote sensing of rice crop areas. *International Journal of Remote Sensing*, 34(6), 2101-2139.
23. Labadarios, D., Mchiza, Z.J.R., Steyn, N.P., Gericke, G., Maunder, E.M.W., Davids, Y.D. and Parker, W.A., 2011. Food security in South Africa: a review of national surveys. *Bulletin of the World Health Organization*, 89, 891-899.
24. Labus, M.P., Nielsen, G.A., Lawrence, R.L., Engel, R. and Long, D.S., 2002. Wheat yield estimates using multi-temporal NDVI satellite imagery. *International Journal of Remote Sensing*, 23(20), 4169-4180.
25. Lamb, D.W. and Brown, R.B., 2001. Pa—precision agriculture: Remote-sensing and mapping of weeds in crops. *Journal of Agricultural Engineering Research*, 78*,* 117-125.
26. Löw, F. and Duveiller, G., 2014. Defining the spatial resolution requirements for crop identification using optical remote sensing. *Remote Sensing*, 6(9), 9034-9063.
27. Moeletsi, M.E. and Walker, S., 2012. Rainy season characteristics of the Free State Province of South Africa with reference to rain-fed maize production. *Water SA*, 38, 775-782.
28. Moulin, S., Bondeau, A. and Delecolle, R., 1998. Combining agricultural crop models and satellite observations: from field to regional scales. *International Journal of Remote Sensing*, 19(6), 1021-1036.
29. NDA, 2002. Provincial Report on Education and Training for Agriculture and Rural Development. National Department of Agriculture. Pretoria.
30. NDA, 2005. Wheat. National Department of Agriculture. Pretoria
31. Prasad, A.K., Chai, L., Singh, R.P., and Kafatos, M., 2006. Crop yield estimation model for Iowa using remote sensing and surface parameters. *International Journal of Applied Earth Observation and Geoinformation*, 8, 26-33.
32. SAGL, 2013. South African Commercial Maize quality 2012/2013. South African Grain Laboratory. Pretoria.

33. Sethi, R.R., Sahu, A.S., Kaledhonkar, M.J., Sarangi, A., Rani, P.R., Kumar, A. and Mandal K.G., 2014. Quantitative determination of rice cultivated areas using geospatial techniques. *IOSR Journal of Environmental Science, Toxicology and Food Technology (IOSR-JESTFT)*, 8, 76-81.
34. Shao, S., Fan, H., Lui, J., Xiao, S., Ross, B., Brisco, R., Brown, R. and Staples, G., 2001. Rice monitoring and production estimation using multitemporal RADARSAT. *Remote Sensing of Environment*, 76, 310-325.
35. Singh, R., Semwal, D., Rai, A. and Chikara, R.S., 2002. Small area estimation of crop yield using remote sensing satellite data. *International Journal of Remote Sensing*, 25, 49-56.
36. Singh, R.P., Roy, S. and Kogan, F., 2003. Vegetation and temperature condition indices from NOAA AVHRR data for drought monitoring over India. *International Journal of Remote Sensing*, 24, 4393–4402.
37. Unganai, L.S. and Kogan, F.N., 1998. Drought Monitoring and Corn Yield Estimation in Southern Africa from AVHRR Data. *Remote Sensing of Environment*, 63, 219-232.

Chapter 2

Evaluating spectral indices for winter wheat health status monitoring

Based on: Mashaba, Z., Chirima, G., Botai, J., Combrinck, L. and Munghemezulu, C., 2016. Evaluating spectral indices for winter wheat health status monitoring in Bloemfontein using Landsat 8 data. *South African Journal of Geomatics*. 5(2), 227-243, http://dx.doi.org/10.4314/sajg.v5i2.10

Abstract

Monitoring wheat growth under different weather and ecological conditions is vital for a reliable supply of wheat yield estimations. Remote sensing techniques have been applied in the agricultural sector for monitoring crop biophysical properties and predicting crop yields. This study explored the application of Land Surface Temperature (LST)-vegetation index relationships for winter wheat in order to determine indices that are sensitive to changes in the wheat health status. The indices were derived from Landsat 8 scenes over the wheat growing area across Bloemfontein, South Africa. The vegetation abundance indices evaluated were the Normalized Difference Vegetation Index (NDVI) and the Green Normalized Difference Vegetation Index (GNDVI). The moisture indices evaluated were the Normalized Difference Water Index (NDWI) and the Normalized Difference Moisture Index (NDMI). The results demonstrated that LST exhibited an opposing trend with the vegetation abundance indices and an analogous trend with the moisture indices. Furthermore, NDVI proved to be a better index for winter wheat abundance as compared to the GNDVI. The NDWI proved to be a better index for determining water stress in winter wheat as compared to the NDMI. These results indicate that NDVI and NDWI are very sensitive to LST. These indices can be comprehensive indicators for winter wheat health status. These pilot results prove that LST-vegetation index relationships can be used for agricultural applications with a high level of accuracy.

Keywords: Wheat, Land Surface Temperature, Indices

2.1. Introduction

Wheat is a staple food for most South Africans after maize, and thus, contributes significantly to the agricultural economy of the country (Meyer and Kirsten, 2005). When the Wheat Board of South Africa was abolished in 1997, wheat markets were deregulated (Meyer and Kirsten, 2005). Consequently, farmers diverted to other economically sustainable crops due to the ensued low profitability of wheat (Breitenbach and Fényes, 2000). Furthermore, climate change and climate variability affected wheat production causing economic instabilities for farmers, especially those in rural communities who depend solely on rain-fed agriculture as their main source of sustenance (Tadross et al., 2005). Subsequently, wheat production declined in South Africa over the years (Breitenbach and Fényes, 2000). The downward trend in production has necessitated monitoring the wheat health status.

Remote Sensing is an essential tool for estimating crop biophysical variables, particularly, the Land Surface Temperature (LST)-vegetation index relationship is related to the canopy health (Huete et al., 1997). However, this relationship has been applied mainly for studying Urban Heat Islands, land use change, and urban expansion (Jiang and Tian, 2010; Guo et al., 2012). Parida et al., (2008) reported that the MODIS derived Soil Moisture Index (SMI) computed from LST-Normalized Difference Vegetation Index (NDVI) relationships is linked to rice yields; low SMI values were associated with a decline in rice productivity. Johnson (2014) linked maize and soybean yields to LST and NDVI for the Corn Belt region in the United States. The study documented that maize and soybean yields were positively correlated with NDVI, and had a negative correlation with daytime LST in the middle of summer. With the application of the LST-vegetation index relationship, water stress and vegetation abundance can be studied earlier during the growing season. This can help farmers modify their irrigation programs or applications of fertilizers, pesticides or herbicides to improve wheat growth at stressed areas. This approach can prevent or minimize crop losses and enhances agricultural productivity.

The aim of this research was to explore indices suitable for monitoring winter wheat health status based on the LST-vegetation index relationship. This application is important because numerous studies have focused on using the LST-NDVI relationship for monitoring global vegetation health or responses of vegetation to drought. However, these studies have not evaluated the performances of other spectral indices for such purposes (Kawabata et al., 2001; Julien et al., 2006; Raynolds et al., 2008; Julien and Sobrino, 2009; Karnieli et al., 2010; Swain et al., 2011; Son et al., 2012). Few studies have focused on using the LST-vegetation index relationship for a specific crop, for example Nemani et al., (1993). Thus, research questions addressed in this study are: can the LST-vegetation relationships be applied for wheat health status monitoring? Which spectral indices are best related to LST for wheat health status monitoring? Moisture indices and vegetation abundance indices derived for Landsat 8 were evaluated against LST. The index sensitive to winter wheat can then be applied in predicting wheat yields in advance before harvesting or even modifying farm management practices during the season for better yields at harvest.

The limitations of the study were that some of the Landsat 8 images were contaminated with cloud cover. Furthermore, because of crop rotations, some of the wheat farmers were not planting wheat at the same places consistently. This limited the samples and Landsat 8 images, which could be analyzed. Although, this study could be extended with a longer time series, the Landsat 8 satellite was only launched recently, in 2013. Another challenge is that optical remote sensing is adversely affected by Precipitable Water Vapour (PWV) in the atmosphere, which can limit the amount of energy recorded by the optical sensor. Thus, reducing the contrast between the visible and near-infrared spectrum (Srivastava et al., 2014). This affects the potential of detecting optimal values for the derived parameters. Most studies do not correct for PWV (e.g., Julien and Sobrino, 2009; Jiang and Tian, 2010; Guo et al., 2012). This correction requires accurate determination of the PWV at the area of interest. Techniques such as Global Navigation Satellite Systems (GNSS) and Radiosondes can provide PWV parameters at millimetre accuracies (Combrink et al., 2007). However, the instrumentation involved are costly to be directly applied to optical remote sensing unless a dedicated campaign is established. As the Trignet Network

increases its density and the GNSS stations are collocated with meteorological stations, PWV values will be easily accessible to the general public (Hackl et al., 2011).

2.2. Background

2.2.1. The phenological growth of wheat

Wheat is grown in winter and summer in South Africa. Winter wheat needs a certain period of cold temperatures between 0 ℃ and 10 ℃ to advance from vegetative growth stage to the flowering stage (anthesis stage). This cold requirement is called vernalisation. Different cultivars of winter wheat need varying periods of vernalisation. Winter wheat requires temperatures varying between 5 ℃ and 25 ℃ throughout the growth cycle (DAFF, 2010). Spring wheat does not require a period of vernalisation as it can be damaged by low temperatures or frost, resulting in lower yields. Spring wheat grows in response to increasing temperature (DAFF, 2010). The ideal temperatures for spring wheat growth are between 22 ℃ and 34 ℃ (DAFF, 2010). In general, wheat requires a rainfall of 600 mm per annum and a soil pH between 6 and 7.5 as it is adversely affected by soils with a high aluminium content during the early stages of development (ARC, 2014). The growth of stages of wheat are detailed in Appendix A1.

2.2.2. The spectral reflectance of vegetation

Through the use of the spectral characteristics of radiation, whether it is reflected, transmitted or absorbed by vegetation, an understanding of physiological responses to growth conditions and plant adaptation to the environment is gained (Lee et al., 2007). The spectral reflectance of green vegetation is distinctive. In the visible part of the electromagnetic spectrum (Figure 3), plants absorb light in the red (620–750 nm) and blue (450–495 nm) bands and reflect more light in the green (495–570 nm) portion.

The main controlling factor is chlorophyll, which is the primary photosynthetic pigment in green plants. In certain instances, when plants are subjected to stresses which

hamper normal growth and chlorophyll production, the absorption decreases in the red and blue regions and the amount of reflection in the red waveband increases (Nandibewoor et al., 2014; Thenkabail et al., 2012; Carter and Knaapp, 2001). The reflectance of vegetation is altered more consistently at the visible wavelengths (~400-750 nm) than the remainder of the incident solar spectrum (Lee et al., 2007).

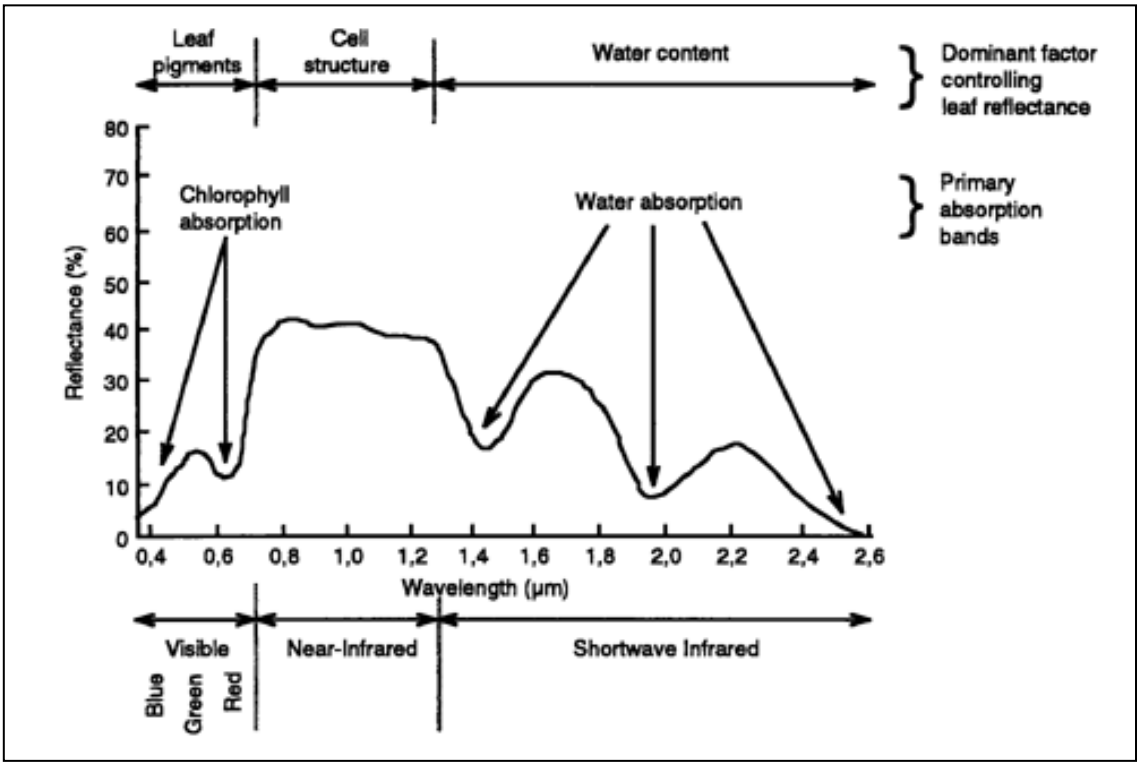

Figure 3. Spectral response characteristics of green vegetation (Source: http://www.r-s-c-c.org/).

In the near infrared region, green vegetation reflects between 40-60 %, this is due to the scattering of light in the intercellular volume of the leaves' mesophyll (Nandibewoor et al., 2014; Thenkabail et al., 2012; Carter and Knaapp, 2001). These reflectance properties of plants in the visible and near infrared portion of the electromagnetic spectrum make it possible to utilize remote sensing techniques.

2.2.3. Spectral indices

Spectral indices (Table 1) make it possible to model relationships between vegetation variables and reflectance data (Cohen et al., 2003). The Normalized Difference Vegetation Index (NDVI) is a commonly used spectral vegetation index. Through the use of the NDVI, crop properties such as leaf biomass, canopy cover, chlorophyll content, nitrogen content, and leaf area are understood (Chavez and Mackinnon, 1994; Gamon et al., 1995). The NDVI is best applied in sparse canopies as it loses its sensitivity in moderate to dense canopies (Gamon et al., 1995).

Table 1. Landsat 8 derived spectral indices utilized in determining the health status of wheat.

Index	Equation	Reference
Normalized Difference Vegetation Index	$NDVI = \frac{B5 - B4}{B5 + B4}$	Elmore et al., (2000)
Green Normalized Difference Vegetation Index	$GNDVI = \frac{B5 - B3}{B5 + B3}$	Moges et al., (2004)
Normalized Difference Water Index	$NDWI = \frac{B3 - B6}{B3 + B6}$	Xu (2006)
Normalized Difference Moisture Index	$NDMI = \frac{B5 - B6}{B5 + B6}$	Jin and Sader (2005)

The Green Normalized Difference Vegetation Index (GNDVI) is a modified version of NDVI, which substitutes the green band in place of the red band in the NDVI equation. The GNDVI is sensitive to the chlorophyll concentration in vegetation when the leaf area index is moderately high. Therefore, the GNDVI overcomes the problems with

saturation, which NDVI exhibits for some vegetation types at later growth stages because it is more sensitive to low chlorophyll concentrations (Gitelson et al., 1996).

The Normalized Difference Water Index (NDWI) is a moisture index for determining vegetation water content (Jackson et al., 2004). The index is designed to enhance the reflectance of water by using the green wavelengths, decreasing the low reflectance of near infrared (NIR) by water features and taking into account that vegetation and soil features have a high reflectance of NIR (McFeeters, 1995).

The Normalized Difference Moisture Index (NDMI) is correlated to the canopy water content and is an indicator of water stress (Hardisky et al., 1983). The NDMI uses the near infrared band, which is used for the detection of reflectance of leaf chlorophyll content, and the mid-infrared band used for detecting the absorbance of leaf moisture (Wilson and Sader, 2002). This index is not as widely applied due to the complexity of interpreting indices that use the mid-infrared band as compared to other indices, which use the red and near-infrared bands (McDonald et al., 1998).

The LST-vegetation index space provides a comprehensive view of vegetation dynamics. There is a negative relationship between LST and vegetation indices (Nemani et al., 1993). This relationship can be applied in studying the spatial variation of LST and vegetation indices for the determination of surface soil moisture or evapotranspiration (Julien and Sobrino, 2009). This is done by deriving drought indices such as the Temperature Dryness Vegetation Index (TDVI) from the LST and NDVI feature space for drought monitoring applications (Sandholdt et al., 2002). The slope of the LST-NDVI is closely related to the evapotranspiration of a surface. Thus, an increase in evapotranspiration causes the soil moisture and NDVI to decline whereas; dense vegetation has more evapotranspiration and a lower LST (Prihodko and Godward, 1997; Boegh et al., 1998). Additionally, the LST-vegetation relationship can be applied for vegetation monitoring (Julien and Sobrino, 2009). This is done by mapping the land cover and land use change patterns (Jiang and Tian, 2010).

2.3. Data and methods

2.3.1. Study area

Bloemfontein covers an area of about 6300 km^2 in the Free State province of South Africa (see Figure 4). The region is semi-arid and experiences summer rainfall from January to March with a mean annual precipitation of approximately 421 mm. Temperatures are low in winter (minimum of -5°C) and high (maximum of 35°C) in summer. The average altitude is less than 1200 m above sea level (Moeletsi, 2011). During the study period, there were 50 farms, which had planted wheat. Of the 50 farms, 24 sample farms had planted wheat in the same area consistently for both years (2013 and 2014). A buffer of 2 km was applied to these 24 sample farms to eliminate samples, which are close to each other, to obtain the final samples depicted in Figure 4.

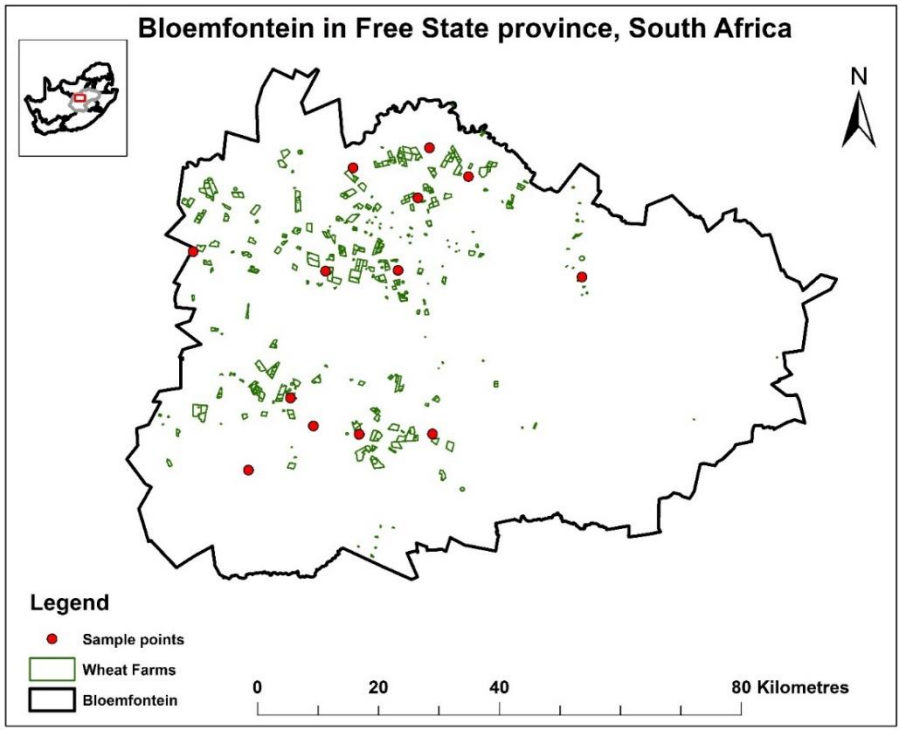

Figure 4. Location map of Bloemfontein within the Free State Province. The sample points are illustrated by the red-dots and the wheat farms are represented by the green polygons.

2.3.2. Data acquisition and data pre-processing

Landsat 8 scenes, depicted in Table 2 for Bloemfontein were acquired from the United States Geological Survey (USGS) site. Landsat 8 images for day of year 180 and 183 for both 2013 and 2014 were selected as wheat is at its greenest during this period. Landsat 8 images were preprocessed by doing radiometric calibration, for the conversion of digital numbers (0 – 255) to radiances. The thermal bands, band 10 (thermal infrared 1) and band 11 (thermal infrared 2) of Landsat 8 were converted to Top of Atmosphere (TOA) spectral radiance for each of the bands using the Interactive Digital Language (IDL) according to:

$$L_{\lambda} = M_{L} Q_{cal} + A_{L} \tag{2.1}$$

where, L_{λ} =TOA spectral radiance (Watts/(m^2*srad*µm)), M_L = Multiplicative rescaling factor for band 10 and 11, Q_{cal} = Satellite image for band 10 and 11 and A_L = Additive rescaling factor for band 10 and 11. The band multiplicative rescaling factor had a constant value of 0.0003342 and a constant additive rescaling factor of 0.1 according to the metadata file for both thermal bands. Atmospheric corrections were done using the Fast Line-of-sight Atmospheric Analysis of Spectral Hypercubes (FLAASH) in the ENVI software, this tool converts the radiance collected at the detector to radiance at the surface (Cooley et al., 2002). These images were used for the computation of Land Surface Temperature.

Reflectance's were computed from the Landsat 8 digital number images to radiometrically calibrate them for the derivation of spectral indices using IDL. The TOA planetary reflectances were computed individually for bands 3 (green), 4 (red), 5 (near infrared) and 6 (short wave infrared 1) using:

$$\rho'_{\lambda} = M_{p} Q_{cal} + A_{p} \tag{2.2}$$

In Equation (2.2), $\rho_{\lambda}^{'}$ = TOA planetary reflectance, M_p = Multiplicative rescaling factor for band 4, 5 and 11, Q_{cal} = Satellite image for band 4, 5 and 11, A_p = Additive rescaling factor for band 4, 5 and 11. Additionally, corrections for the sun angle had to be made, according to:

$$\rho_{\lambda} = \frac{\rho_{\lambda}^{'}}{(\sin\theta_{SE})} \tag{2.3}$$

where, ρ_{λ} = TOA planetary reflectance with correction for sun angle, $\rho_{\lambda}^{'}$ = TOA planetary reflectance and θ_{SE} = Sun elevation angle.

Table 2. Landsat 8 scenes for Bloemfontein selected for the study (Source: http://earthexplorer.usgs.gov/).

Path/row	DOY	Latitude	Longitude	Sun elevation (°)	Scene cloud cover (%)
171/80	180	-28.8691	26.22283	29.71951	0.03
171/80	183	-28.8691	26.22283	29.53000	2.63

2.3.3. Computing the Land Surface Temperature and Vegetation indices

The TOA radiance images (L_{λ}) were used to calculate the brightness temperature. However, both images had different values for the thermal conversion constants according to the metadata file; these were taken into account during the computation. The brightness temperature (T_B) was calculated individually for both band 10 and band 11 according to:

$$T_B = \frac{K_2}{\left(\frac{K_1}{L_{\lambda}} + 1\right)} \tag{2.4}$$

where, K_2 =Thermal conversion constant (band 10 = 1321.08 and band 11 = 1201.14), K_1 = Thermal conversion constant (band 10 = 774.89 and band 11 = 480.89) and L_λ = TOA spectral radiance (Watts/(m^2*srad*µm)). Thereafter, the land surface temperature (T_s) was computed for band 10 and band 11 separately using the brightness temperature images (Equation 2.4) according to Artis and Carnahan (1982):

$$T_s = \frac{T_B}{1+(\lambda T_B/\alpha)\ln\varepsilon} \tag{2.5}$$

where, λ = Wavelength of emitted radiance (11.5x10^{-6}m), $\alpha = hc/\delta$, h = Planck constant (6.626x10^{-34}Js), c = Velocity of light (2.998x10^{8}m/s), δ = Boltzmann constant (1.38x10^{-23}J/K), ε = Surface emissivity. The emissivity had to be taken into account, this was assumed to be 0.99 because NDVI falls between the range of (0.2< NDVI > 0.5) (Sobrino et al., 2004), hence, the fractional vegetation proportion (Pv) was not necessary to calculate.

$$\varepsilon = \begin{cases} 0.990 & (NDVI < 0.2,\ NDVI > 0.5) \\ 0.004Pv + 0.986 & (0.2 \le NDVI \le 0.5) \end{cases} \tag{2.6}$$

The NDVI, GNDVI, NDWI and NDMI spectral indices were computed from the reflectance images ρ'_λ using IDL according to Table 1.

2.3.4. Statistical analysis

Least squares linear regression models were developed in R-Studio for the LST-vegetation index relationships. The LST was considered a dependent variable and the spectral indices were considered independent variables. The coefficient of determination (R^2) was calculated to determine the fit of the linear models. The p-value was calculated to determine the significance of the relationships. The Root Mean Square Error (RMSE) to evaluate the validity of the models. Thereafter, the scatterplots were made to understand the LST-vegetation index slope and the distribution of the sample points.

2.4. Results and discussion

2.4.1. Spatial variation of the LST-vegetation index relationships at a farm level

The spatial distribution of LST and the vegetation indices for selected winter wheat farms are illustrated in Figure 5. The LST is low at vegetated wheat farms, whereas, the NDVI and GNDVI are high at these wheat farms, the opposite trend is observed for fallow or harvested farms. This observation is expected for wheat; healthy vegetation reflects more radiation in the near infrared section of the solar spectrum as compared to the visible section. Additionally, healthy vegetation emits less thermal radiation in the infrared section because of cooler transpiration from the canopy (Kogan et al., 2005). The moisture indices are positively related to LST and indicate that wheat farms, which are flourishing have a high moisture content. Since Bloemfontein is characterized by summer rainfall, this could be indicative that these areas have a higher residual soil moisture during the winter season because of a high water table. These qualitative relationships were verified statistically.

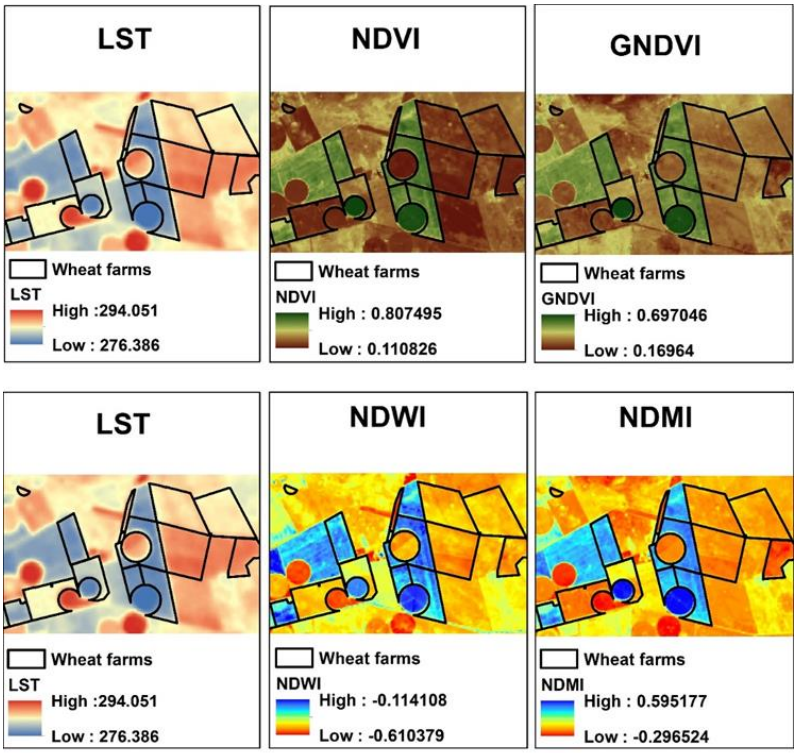

Figure 5. The performance of each vegetation index at a farm level for winter wheat. The farms were selected as examples from the wheat farms in Figure 1.

2.4.2. Statistical analysis of the LST-vegetation index relationships

The results of regression analysis between LST and vegetation indices are depicted in Table 3. Through the use of R^2, moderate relationships were observed between LST and NDVI for the selected vegetation indices. The LST and NDWI exhibited a strong relationship for the selected moisture indices. The LST-GNDVI and LST-NDMI both had a moderate relationship. This indicated that the LST-NDVI and the LST-NDWI were better estimates of the wheat health status. The relationships were not the same over the years; this could be a result of changes in the soil conditions due to agricultural management practices and fluctuations in the weather patterns. Significance levels were calculated in order to determine the relationship between LST and the vegetation indices. Most of the derived linear relationships indicated a good level of significance with p-values less than 0.05 for all the years (Table 3). The RMSE values were lower in 2014 compared to 2013, this indicated improvements in the accuracy of the models.

The scatterplots in Figure 6 are for the winter wheat sample points displayed in Figure 4. The scatterplots indicate a decrease in the wheat health status from 2013 to 2014 because the values for LST and the spectral indices for the sample points decreased over these years. Steeper slopes on the LST-vegetation index plots are observed on periods of reduced soil moisture and vegetation amount (Goetz, 1997). The slope of the LST-vegetation index scatterplots were negative, consistent with previous research. Nemani et al., (1993) observed a negative relationship between NDVI and LST for grasses, crops, and forests, and established that fractional canopy cover was an important variable in controlling surface temperatures. Hope (1988) observed a negative relationship when determining the actual canopy resistance for wheat by combining the remotely sensed spectral reflectance and land surface temperature. Weng et al., (2004) observed a negative relationship between cropland and land surface temperature. These relationships arise due to the cooling effects of canopy transpiration (Kogan et al., 2005). The use of the LST-vegetation relationships for crop health status monitoring described in this research can be used to replace the Crop Water Stress Index (CWSI), which is more computationally intensive as it requires the computation of the vegetation index-temperature trapezoid (Moran et al., 1994; Clarke,

1997). However, the disadvantage of using satellite remotely sensed imagery is that they give an indication of the crops water status only during the time the image was taken, therefore, it is important to select an image at the critical growth stages. To overcome this problem in time delay, Unmanned Aerial Vehicles (UAVs) can be used. Overall, this research has proven that the LST-vegetation index relationships can be used for wheat health status monitoring and has determined the best indices, which comprehensively describe wheat health.

Table 3. The LST-vegetation index regression models, coefficient of determination (R^2) and significance level for winter wheat.

Relationship	Year	Regression Model	R^2	Significance(p-value)
LST-NDVI	2013	LST=-8.890*NDVI+289	0.3552	0.031600
	2014	LST=-9.841*NDVI+292	0.6200	0.001400
LST-GNDVI	2013	LST=-15.462*GNDVI+293	0.2810	0.062380
	2014	LST=-12.485*GNDVI+294	0.4124	0.017195
LST-NDWI	2013	LST=-25.734*NDWI+275	0.6502	0.000870
	2014	LST=-19.110*NDWI+281	0.8949	0.000001
LST-NDMI	2013	LST=-9.855*NDMI+286	0.5269	0.004970
	2014	LST=-8.256*NDMI+289	0.7916	0.000040

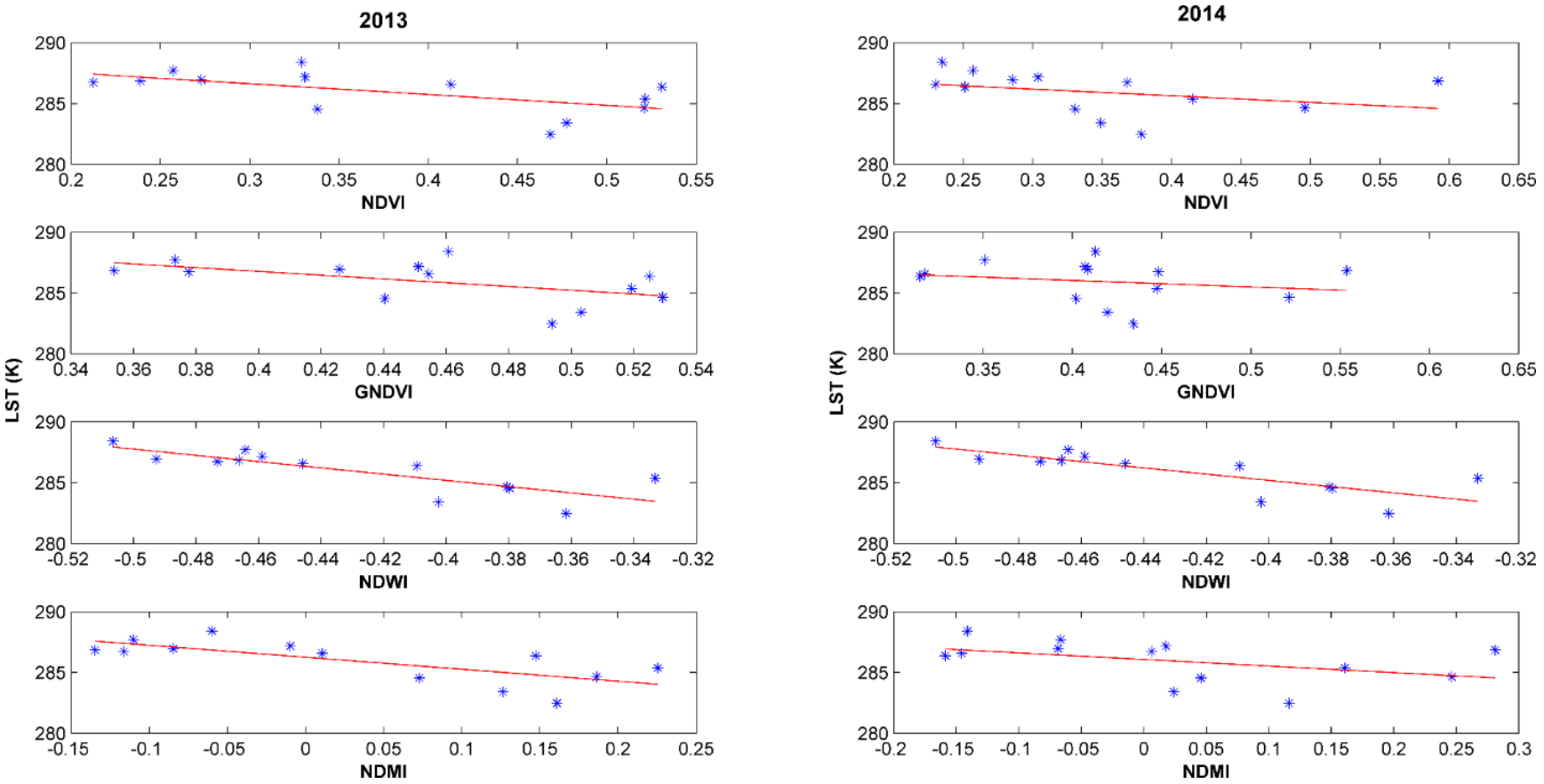

Figure 6. The LST-vegetation index scatter plots for 2013-2014 at the selected sample points. The LST-vegetation index plots have negative relationships.

2.5. Conclusion

This research was important because wheat is one of the staple crops for South Africa. With Landsat 8 derived remotely sensed data, the indices sensitive to changes in wheat health were identified. The LST has an inverse relationship with the vegetation abundance indices; this indicates that healthy wheat releases more transpiration as compared to unhealthy wheat. The NDVI and NDWI were found to be suitable indices for monitoring the wheat health status as compared to the GNDVI and NDMI. A better fit was observed for the moisture indices as compared to the vegetation abundance indices. To improve these findings, more sample points can be added depending on how consistently farmer's plant wheat at the same areas. The performance of other vegetation indices can be compared with the ones used in this research. These pilot results indicate that the LST-vegetation index relationships can be applied to monitor wheat health status in the Bloemfontein area at the critical stages of growth. Using the LST-vegetation index relationship, farmers can mitigate conditions hampering wheat growth such as a lack of moisture, fertilizer, pesticides or herbicides at stressed areas.

2.6. References

1. ARC, 2014. Guideline for the production of small grains in the summer rainfall areas. University of Free State. Free State.
2. Artis, D.A. and Carnahan, W.H., 1982. Survey of emissivity variability in thermography of urban areas. *Remote Sensing of Environment*, 12(4), 313-329.
3. Boegh, E., Soegaard, H., Hanan, H., Kabat, P. and Lesch, L., 1998. A remote sensing study of the NDVI-Ts relationship and the transpiration from sparse vegetation in the Sahel based on high resolution data. *Remote Sensing Environment,* 69, 224 – 240.
4. Breitenbach, M.C. and Fényes, T.I., 2000. Maize and wheat production trends in South Africa in a deregulated environment. *Agrekon*, 39, 292-312.
5. Carter, G.A. and Knapp, A.K., 2001. Leaf optical properties in higher plants: linking spectral characteristics to stress and chlorophyll concentration. *American Journal of Botany*, 88(4), 677-684.
6. Chavez, P.S. and MacKinnon, D.J., 1994. Automatic detection of vegetation changes in the southwestern United States using remotely sensed images. *Photogrammetric Engineering and Remote Sensing*, 60(5), 571-583.
7. Clarke, T.R., 1997. An empirical approach for detecting crop water stress using multispectral airborne sensors. *HortTechnology*, 7(1), 9-16.
8. Cohen, W.B., Maiersperger, T.K., Gower, S.T. and Turner, D.P., 2003. An improved strategy for regression of biophysical variables and Landsat ETM+ data. *Remote Sensing of Environment*, 84(4), 561-571.
9. Combrink, A.Z., Bos, M.S., Fernandes, R.M., Combrinck, W.L. and Merry, C.L., 2007. On the importance of proper noise modelling for long-term precipitable water vapour trend estimations. *South African Journal of Geology*, 110(2-3), 211-218.
10. Cooley, T., Anderson, G.P., Felde, G.W., Hoke, M.L., Ratkowski, A.J., Chetwynd, J.H., Gardner, J.A., AdlerGolden, S.M., Matthew, M.W., Berk, A. and Bernstein, L., 2002. FLAASH, a MODTRAN4-based atmospheric correction algorithm, its application and validation, In Geoscience and Remote Sensing Symposium, 2002. IGARSS'02. 2002 IEEE International, 3, 1414-1418.
11. DAFF, 2010. Wheat production guideline. Department of Agriculture Forestry and Fisheries. Pretoria.
12. Elmore, A.J., Mustard, J.F., Manning, S.J. and Lobell, D.B., 2000. Quantifying vegetation change in semiarid environments: precision and accuracy of spectral mixture analysis and the normalized difference vegetation index. *Remote Sensing of Environment*, 73(1), 87-102.
13. Gamon, J.A., Field, C.B., Goulden, M.L., Griffin, K.L., Hartley, A.E., Joel, G., Peñuelas, J. and Valentini, R., 1995. Relationships between NDVI, canopy structure, and photosynthesis in three Californian vegetation types. *Ecological Applications*, 5(1), 28-41.

14. Gitelson, A.A., Kaufman, Y.J. and Merzlyak, M.N., 1996. Use of a green channel in remote sensing of global vegetation from EOS-MODIS. *Remote Sensing of Environment*, 58(3), 289-298.
15. Goetz, S.J., 1997. Multi-sensor analysis of NDVI, surface temperature and biophysical variables at a mixed grassland site. *International Journal of Remote Sensing*, 18(1), 71-94.
16. Guo, Z., Wang S.D., Cheng, M.M. and Shu, Y., 2012. Assessing the effect of different degrees of urbanization on land surface temperature using remote sensing images. *Procedia Environmental Sciences*, 13, 935-942.
17. Hackl, M., Malservisi, R., Hugentobler, U. and Wonnacott, R., 2011. Estimation of velocity uncertainties from GPS time series: Examples from the analysis of the South African TrigNet network. *Journal of Geophysical Research: Solid Earth*, 116(B11404).
18. Hardisky, M.A., Klemas, V. and Smart, R.M., 1983. The influence of soil salinity, growth form, and leaf moisture on the spectral radiance of Spartina alterniflora canopies. *Photogrammetric Engineering and Remote Sensing*, 49, 77-83.
19. Hope, A.S., 1988. Estimation of wheat canopy resistance using combined remotely sensed spectral reflectance and thermal observations. *Remote Sensing of Environment*, 24(2), 369-383.
20. Huete, A.R., Liu, H.Q., Batchily, K. and Van Leeuwen, W.J.D.A., 1997. A comparison of vegetation indices over a global set of TM images for EOS-MODIS. *Remote Sensing of Environment*, 59, 440-451.
21. Jackson, T.J., Chen, D., Cosh, M., Li, F., Anderson, M., Walthall, C., Doriaswamy, P. and Hunt, E.R., 2004. Vegetation water content mapping using Landsat data derived normalized difference water index for corn and soybeans. *Remote Sensing of Environment*, 92(4), 475-482.
22. Jiang, J. and Tian, G. 2010. Analysis of the impact of Land use/Land cover change on Land Surface Temperature with Remote Sensing. *Procedia Environmental Sciences*, 2, 571-575.
23. Jin, S. and Sader, S.A., 2005. Comparison of time series tasseled cap wetness and the normalized difference moisture index in detecting forest disturbances. *Remote Sensing of Environment*, 94(3), 364-372.
24. Johnson, D.M., 2014. An assessment of pre-and within-season remotely sensed variables for forecasting corn and soybean yields in the United States. *Remote Sensing of Environment*, 141, 116-128.
25. Julien, Y., Sobrino, J.A. and Verhoef, W., 2006. Changes in land surface temperatures and NDVI values over Europe between 1982 and 1999. *Remote Sensing of Environment*, 103(1), 43-55.
26. Julien, Y. and Sobrino, J.A., 2009. The Yearly Land Cover Dynamics (YLCD) method: An analysis of global vegetation from NDVI and LST parameters. *Remote Sensing of Environment*, 113(2), 329-334.

27. Karnieli, A., Agam, N., Pinker, R.T., Anderson, M., Imhoff, M.L., Gutman, G.G., Panov, N. and Goldberg, A., 2010. Use of NDVI and land surface temperature for drought assessment: Merits and limitations. *Journal of Climate*, 23(3), 618-633.
28. Kawabata, A., Ichii, K. and Yamaguchi, Y., 2001. Global monitoring of interannual changes in vegetation activities using NDVI and its relationships to temperature and precipitation. *International Journal of Remote Sensing*, 22(7), 1377-1382.
29. Kogan, F., Yang, B., Wei, G., Zhiyuan, P. and Xianfeng, J., 2005. Modelling corn production in China using AVHRR-based vegetation health indices. *International Journal of Remote Sensing*, 26(11), 2325-2336.
30. Lee, K.S., Kook, M.J., Shin, J.I., Kim, S.H. and Kim, T.G., 2007. Spectral characteristics of forest vegetation in moderate drought condition observed by laboratory measurements and spaceborne hyperspectral data. *Photogrammetric Engineering & Remote Sensing*, 73(10), 1121-1127.
31. McDonald, A.J., Gemmell, F.M. and Lewis, P.E., 1998. Investigation of the utility of spectral vegetation indices for determining information on coniferous forests. *Remote Sensing of Environment*, 66(3), 250-272.
32. McFeeters, S.K., 1995. The use of the Normalized Difference Water Index (NDWI) in the delineation of open water features. *International Journal of Remote Sensing*, 17(7), 1425-1432.
33. Meyer, F. and Kirsten, J., 2005. Modelling the wheat sector in South Africa, *Agrekon*, 44, 225-237.
34. Moges, S.M., Raun, W.R., Mullen, R.W., Freeman, K.W., Johnson, G.V. and Solie, J.B., 2004. Evaluation of green, red, and near infrared bands for predicting winter wheat biomass, nitrogen uptake, and final grain yield. *Journal of Plant Nutrition*, 27(8), 1431-1441.
35. Moran, M.S., Clarke, T.R., Inoue, Y. and Vidal, A., 1994. Estimating crop water deficit using the relation between surface-air temperature and spectral vegetation index. *Remote Sensing of Environment*, 49(3), 246-263.
36. Nandibewoor, A., Adiver, P. and Hegadi, R., 2014. Identification of vegetation from Satellite derived Hyper Spectral Indices. *IEEE*, 1215-1219.
37. Nemani, R., Pierce, L., Running, S. and Goward, S., 1993. Developing satellite-derived estimates of surface moisture status. *Journal of Applied Meteorology*, 32(3), 548-557.
38. Parida, B.R., Collado, W.B., Borah, R., Hazarika, M.K. and Samarakoon, L., 2008. Detecting drought-prone areas of rice agriculture using a MODIS-derived soil moisture index. *GIScience & Remote Sensing*, 45(1), 109-129.
39. Prihodko, L. and Goward, S.N., 1997. Estimation of air temperature from remotely sensed surface observations. *Remote Sensing of Environment*, 60(3), 335-346.
40. Raynolds, M.K., Comiso, J.C., Walker, D.A. and Verbyla, D., 2008. Relationship between satellite-derived land surface temperatures, arctic vegetation types, and NDVI. *Remote Sensing of Environment*, 112(4), 1884-1894.

41. Sandholt, I., Rasmussen, K. and Andersen, J., 2002. A simple interpretation of the surface temperature/vegetation index space for assessment of surface moisture status. *Remote Sensing of Environment*, 79(2), 213-224.
42. Sobrino, J.A., Jiménez-Muñoz, J.C. and Paolini, L., 2004. Land surface temperature retrieval from LANDSAT TM 5. *Remote Sensing of Environment*, 90(4), 434-440.
43. Son, N.T., Chen, C.F., Chen, C.R., Chang, L.Y. and Minh, V.Q., 2012. Monitoring agricultural drought in the Lower Mekong Basin using MODIS NDVI and land surface temperature data. *International Journal of Applied Earth Observation and Geoinformation*, 18, 417-427.
44. Srivastava, P.K., Han, D., Rico-Ramirez, M.A., Bray, M., Islam, T., Gupta, M. and Dai, Q., 2014. Estimation of land surface temperature from atmospherically corrected LANDSAT TM image using 6S and NCEP global reanalysis product. *Environmental Earth Sciences*, 72(12), 5183-5196.
45. Swain, S., Wardlow, B.D., Narumalani, S., Tadesse, T. and Callahan, K., 2011. Assessment of vegetation response to drought in Nebraska using Terra-MODIS land surface temperature and normalized difference vegetation index. *GIScience & Remote Sensing*, 48(3), 432-455.
46. Tadross, M.A., Hewitson, B.C. and Usman, M.T., 2005. The interannual variability of the onset of the maize growing season over South Africa and Zimbabwe. *Journal of Climate*, 18, 3356-3372.
47. Thenkabail, P.S., Lyon, J.G. and Huete, A., 2012. Hyperspectral remote sensing of vegetation, CRC Press, London, United Kingdom, 293.
48. Weng, Q., Lu, D. and Schubring, J., 2004. Estimation of land surface temperature–vegetation abundance relationship for urban heat island studies. *Remote Sensing of Environment*, 89(4), 467-483.
49. Wilson, E.H. and Sader, S.A., 2002. Detection of forest harvest type using multiple dates of Landsat TM imagery. *Remote Sensing of Environment*, 80(3), 385-396.
50. Xu, H., 2006. Modification of normalised difference water index (NDWI) to enhance open water features in remotely sensed imagery. *International Journal of Remote Sensing*, 27(14), 3025-3033.

Chapter 3

Forecasting dryland winter wheat yields using MODIS NDVI data

Based on: Mashaba, Z., Chirima, G., Botai, J., Combrinck, L., Munghemezulu, C and Dube, E., 2016. Forecasting winter wheat yields using MODIS NDVI data for the Central Free State Region. *South African Journal of Science.* (Accepted, manuscript ID: SAJS-2016-0201.R2)

Abstract

Consumption of wheat is widespread and increasing in South Africa. However, global wheat production is projected to decline. Hence, wheat yield forecasting is crucial for ensuring food security for the country. The objectives of this study were to investigate whether the anthesis wheat growth stage was suitable for forecasting dryland wheat yields in Central Free State using satellite imagery and linear predictive modelling. Ten years of Normalized Difference Vegetation Index (NDVI) data smoothed with a Savitsky-Golay filter and ten years of wheat yield data were used for model calibration. Diagnostic plots and statistical procedures were used for model validation and assessing model adequacy. The period 30 days before harvest during the anthesis stage was established to be the best period to use the linear regression model. The calibrated model had a coefficient of determination of (R^2) value of 0.73, p-value of 0.00161 and a Root Mean Squared Error (RMSE) of 0.41 ton ha^{-1}. Residual plots confirmed that a linear model had a good fit for the data. The quantile-quantile (Q-Q) plot provided evidence that the residuals were normally distributed. This meant that assumptions of linear regression were fulfilled and hence, the model can be used as a forecasting tool. Model validation showed high levels of accuracy. The evidence indicates that use of Moderate Resolution Imaging Spectroradiometer (MODIS) data during the anthesis growth stage is reliable, cost effective, and could be a time saving alternative to ground based surveys when forecasting dryland wheat yields in Central Free State.

Keywords: dryland wheat, wheat yield, NDVI, MODIS, food security

3.1. Introduction

Wheat (*Triticum aestivum L*.) is an important crop in many parts of the world including South Africa, where it is the second largest component of the staple diet after maize (Breitenbach and Fenyes, 2000; Ren et al., 2008). Consequently, it is crucial to predict wheat yields as global wheat production is expected to decrease under conventional management due to climate variability (Parry et al., 2004; Ortiz et al., 2008). Additionally, a challenge exists to feed a growing human population while avoiding environmental problems such as deforestation and land degradation (Balkovič et al., 2014). The Central Free State province of South Africa is a land locked, dryland wheat production region, which exhibits variable agricultural production due to droughts, a reduced capacity to operate in world markets owing to high transport costs and foreign exchange constraints (Hammer et al., 2001; Byerlee et al., 2006). In order to ensure food security, there is a need for generating timely and accurate information on crop yields (Becker-Reshef et al., 2010). This section focuses on the development of a reliable, large scale estimate of wheat yields using the Moderate Resolution Imaging Spectroradiometer–Normalized Difference Vegetation Index (MODIS-NDVI). Accurate forecasting of the yield potential of dryland wheat in the Central Free State will aid agricultural decision makers in balancing the trade of agricultural commodities and reducing short-term price instabilities (Bastiaanssen et al., 2003).

Commonly, yield-forecasting models are more reliable if applied during specific critical plant growth stages. For wheat, the anthesis stage (flowering stage), appears to be an important stage (Aparicio et al., 2002; Moriondo et al., 2007; Lopresti et al., 2015). During this time, water deficiencies lead to yield losses via reducing the spike and spikelet numbers, as well as fertility of the remaining spikelets (Giunta et al., 1993). Water shortages during this stage also accelerates leaf senescence and reduces the rate of grain filling, and thus, consequently, reducing the mean kernel weight (Royo et al., 1999). High temperature reduces the number of grains per ear, kernel weight and harvest index, leading to reduced grain yields (Wheeler et al., 1996).

However, a few studies have been done on using remote sensing data for yield estimation in South Africa (Unganai and Kogan, 1998; Frost et al., 2013). For example, Unganai and Kogan, (1998) demonstrated that maize yields can be estimated using Advanced Very High Resolution Radiometer (AVHRR) data with a spectral resolution of 0.58-12.5 micrometres. In that study, it was found that Vegetation Condition Index (VCI) and Temperature Condition Index (TCI) derived from AVHRR data were highly correlated with maize yields. Frost et al., (2013) demonstrated that Terra MODIS (0.6-1.1 micrometres) satellite sensor data products can be applied for maize yield estimation in South Africa. In that study, the window method was utilized and the resulting window periods showed that average NDVI and average Enhanced Vegetation Index (EVI) data can be used for maize yield estimations.

There is a need for more studies to be done in South Africa using remote sensing for yield predictions. This is important because wheat production is decreasing due to weather variability within summer rainfall areas, the deregulation of the wheat industry, and farmers converting to sustainable crops (i.e. soybean and canola) (Breitenbach and Fenyes, 2000). Furthermore, timeous generation of yield projections will support timeous decisions concerning either importation or exportation of wheat. Therefore, the overall objective of this section is to develop a large scale yield model for dryland winter wheat for the Central Free State production region using MODIS data. This was done by investigating whether wheat yields in Central Free State are correlated with the MODIS-NDVI during the anthesis stage (Aparicio et al., 2002; Moriondo et al., 2007; Lopresti et al., 2015), and validating the performance and adequacy of the calibrated model.

3.2. Background

3.2.1. Remote sensing for crop yield prediction

Vegetation indices derived from remote sensing technology are often used for crop monitoring and crop yield estimates (Ren et al., 2008). This technique is based on the assumption that spectral data are related to canopy reflectance parameters which in turn, are related to the final yield (Carlson and Ripley, 1997; Singh et al., 2002). The Normalized Difference Vegetation Index (NDVI) used in this study, is an indicator of

the photosynthetic potential of a vegetation canopy (Reed et al., 1994). The NDVI makes use of the near infrared (NIR) band and visible red band in the electromagnetic spectrum (Tucker, 1979). The limitation of this index is that it gets saturated in areas with dense biomass, however, hyperspectral data can overcome this limitation (Asner et al., 2003; Chen et al., 2006). However, hyperspectral imaging is costly as it requires a dedicated campaign, has a limited extent and a complex data structure compared to MODIS data, which is freely available.

Numerous studies have used NDVI derived from various remotely sensed images for crop yield estimations (Yang et al., 2006; Nuarsa et al., 2011; Mutanga et al., 2013). For example, Yang et al., (2006) evaluated the accuracy of QuickBird satellite imagery and airborne imagery for mapping grain sorghum yield patterns. The results illustrated that Quickbird and airborne imagery had similar correlations with grain yield at 2.8 and 8.4 m resolutions. Nuarsa et al., (2011) estimated rice yields using an exponential model derived from Landsat Enhanced Thematic Mapper plus (ETM+) NDVI and field observed rice yield in the Tabanan Regency. The study observed a coefficient of determination (R^2) and standard error (SE) of 0.852 and 0.077 tons ha^{-1} respectively. Mutanga et al., (2013) determined the optimal time for predicting sugarcane yield to be two months before harvest using NDVI derived from SPOT images.

3.2.2. The Moderate Resolution Imaging Spectroradiometer vegetation products

The MODIS instrument, mounted on board the Terra and Aqua satellites collects data in 36 spectral bands to provide global coverage of the land, ocean and atmosphere (Wu et al., 2010; Salomonson et al., 1989). Data acquired by MODIS are intended for the continuity of the AVHRR time series of 20 years at an improved spatial resolution (250 m–1 km), spectral resolution (36 bands), temporal resolution (1-2 days) and geolocation accuracy (Gallo et al., 2005; Wolfe et al., 2002). Additionally, MODIS has a better cloud screening and atmospheric correction system (Justice et al., 1998).

The MODIS land products include: vegetation indices, leaf area index, fraction of photosynthetically active radiation, bidirectional reflectance distribution function, land surface temperature, fire, net primary productivity, land cover/use change and snow

(Justice et al., 1998). The MODIS vegetation index product is reviewed in this section, further details on the MODIS bands and uses are in Appendix A4. The standard vegetation index products are provided at 250 m, 500 m, 1 km and 0.05° (5600 m) resolutions by means of 16-day composites. The two MODIS vegetation index products are the NDVI and the EVI given by Equation (3.1) and Equation (3.2):

$$NDVI = \frac{NIR - \mathrm{Re}\,d}{NIR + \mathrm{Re}\,d}, \tag{3.1}$$

$$EVI = G\frac{\rho_{\mathrm{NIR}} - \rho_{red}}{\rho_{NIR} + C_1 \times \rho_{red} - C_2 \times \rho_{blue} + L}, \tag{3.2}$$

where, G is the gain factor, ρ is the reflectance, L is the canopy background adjustment, C_1 and C_2 are coefficients related to aerosol correction, EVI is sensitive to high biomass areas and dense forest regions. The blue band for EVI is derived from the 500 m blue band surface reflectance because there is no 250 m blue band for the MODIS instrument (Huete et al., 2002).

Composting techniques are applied to the MODIS vegetation index products to remove the effects of clouds, aerosols and cloud shadows. There are three composting techniques applied to MODIS data, namely, the maximum value composting (MVC), constrained view maximum value composting (CV-MVC) and bidirectional reflectance distribution function (BRDF). These techniques were developed based on the experiences from the AVHRR-NDVI composting algorithm. The AVHRR-NDVI selects the maximum NDVI value per pixel at 14-day intervals, this is referred to as MVC. This technique decreases atmospheric effects; data quality checks are also included during the procedure (Wang et al., 2002). However, this method selects pixels, which have larger viewing angles and sun angles that are not always cloud free, atmospherically clear or closest to nadir (Goward et al., 1991).

The CV-MVC method is also used for composting MODIS vegetation data products. This technique compares two highest NDVI values and selects the observation closest to nadir to represent the 16-day composite cycle. The use of CV-MVC aids in reducing

the spatial and temporal discontinuities in the composted product. There is no different method used for composting EVI, both products are derived using the same pixel observation (Huete, 2002).

The BRDF model is used to interpolate nadir-equivalent band reflectance values from all bidirectional reflectance observations, which have an acceptable quality for the computation of vegetation indices. The Walthall BRDF model (Walthall et al., 1985) is used when there are five clear pixels. The criteria used by MODIS for composting is to first use the CV-MVC method if there are less than five acceptable pixel values, the BRDF composite model is used when there are at least five clear pixels or the MVC method is used if none of the observations are acceptable (Huete, 2002).

3.3. Data and methods

3.3.1. Study Area

The Free State province hosts four distinct dryland wheat production regions: Central Free State, North Western Free State, South Western Free State, and Eastern Free State (Hensley et al., 2006; ARC, 2014). These regions receive summer rainfall and experience frequent droughts. Therefore, farmers adopt farm management practices, which make efficient use of rain for crop production. The underlying geology of the Free State are rocks from the Beaufort and Ecca Groups of the Karoo Supergroup, which make up the parent material for the soils (Hensley et al., 2006). The study sites, Arlington, Tweespruit and Excelsior are in the Central Free State Production Region (Figure 7). These sites are part of the National Wheat Cultivar Evaluation Programme (NWCEP) conducted by the Agricultural Research Council Small Grains Institute (ARC-SGI). The programme delivers information about the performance of wheat varieties from the major breeding companies of South Africa. The sites were selected systematically in a manner such that they are representative of all the production conditions of this geographic region (Dube et al., 2015). Dryland wheat planting normally takes place from the first week of July (ARC, 2014).

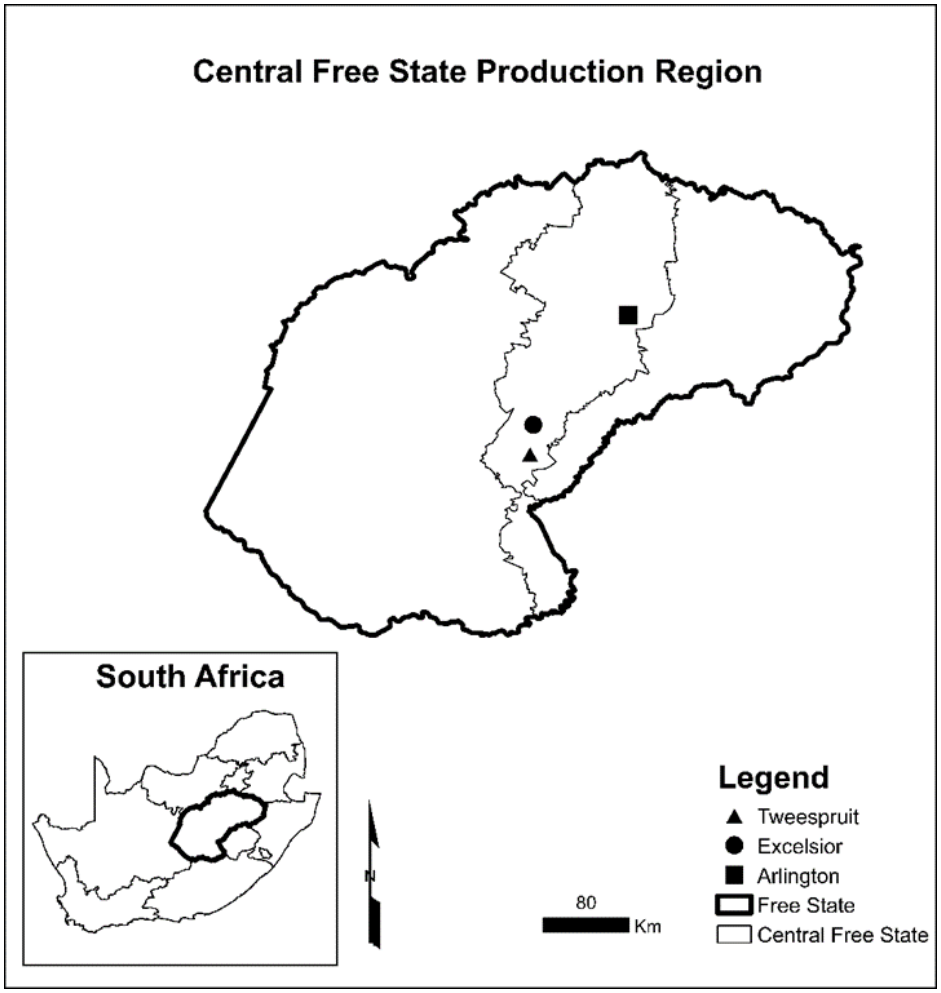

Figure 7. Map of the Central Free State wheat production region depicting the three study sites.

3.3.2. MODIS-NDVI

The 16-day composite MODIS NDVI (MOD13Q1) product images with a 250 m resolution used in this study are freely available from the National Aeronautical Space Agency (NASA) Earth Observing System (EOS) website. The data were obtained for a ten-year period from 2000 to 2013 (excluding 2001/2002/2008/2011) based on the available wheat yield data collected for at the study sites. The MOD13Q1 product is computed from the surface reflectance of each band (red and near infrared) as it would have been measured at ground level if there was no atmospheric scattering or absorption (Vermote et al., 2002). During data processing, corrections are made for the effects of atmospheric gases, aerosols and thin cirrus clouds (Vermote et al., 1997).

The downloaded MODIS-NDVI images were reprojected from Sinusoidal Projection to Geographic Projection using the MODIS Reprojection Tool (Dwyer and Schmidt, 2006). Additionally, rescaling of the raster images had to be done to correct the range of NDVI values to range from -1 to 1. The raster images were cropped with the wheat boundaries obtained from the ARC in collaboration with Geo Terra Image (GTI) and Spatial Business Intelligence (SIQ). The values for NDVI were extracted for each of the wheat boundary pixels at the three localities.

3.3.3. Wheat yield data

Annual wheat yield data for ten seasons (2000-2013 excluding 2001/2002/2008/2011) were used for this study. These data were collected by the ARC-SGI under the NWCEP programme. A randomised complete block design was used for the entire trials layout. The trials are planted inside non-irrigated wheat fields, in line with crop management practices with regard to tillage practices, seeding rates, weed control, fertilizer application, pest and disease control as well as planting date. The dryland wheat trials consist of five rows that are 5 m long with an inter-row spacing of 0.45 m. The harvest area is 5 × 1.35 m^2, represented by three central rows. In order to adequately test the cultivars on the planting date spectrum, which is as wide as three months, two independent randomised trials (early and late planting) are planted at all sites within geographic regions.

3.3.4. Savitzky-Golay filter: applied to NDVI time-series

The Savitzky-Golay (S-G) (Savitzky and Golay, 1964) filter algorithm was used to smooth out the MODIS-NDVI data. The S-G filter is based on local least-squares polynomial approximation. The advantages of the S-G filter are that it preserves features of the data such as relative maxima, minima and widths (Kim et al., 2014). The S-G smoothing algorithm is given in Equation (3.3):

$$Y_j^* = \frac{\sum_{i=-m}^{i=m} C_i Y_{j+i}}{N} \quad (3.3)$$

where, Y_j^* is the filtered value, C_i is the coefficient for the i-th NDVI value of the filter, Y_{j+1} represents the original NDVI value, and N is the number of convoluting integers equal to smoothing window size (2m+1) (Savitzky and Golay, 1964). The larger the value of m, the smoother the results at the expense of flattening sharp peaks (Kim et al., 2014).

3.3.5. Model development

A linear regression model was developed between the average yield of different late planted wheat cultivars (this is the observed yield) and the average NDVI for the three study sites. The average yield was considered an independent variable and the average NDVI was considered a dependent variable according to:

$$P(Y \mid x) = \beta_0 x + \beta_1 \quad (3.4)$$

where, $P(Y \mid x)$ is the predicted yield as function of NDVI, x is the NDVI, β_0 is the coefficient and β_1 is the constant for winter wheat yield. Different models (logarithmic, exponential and power) were compared for the purpose of evaluating the models so that the best fitting model is selected (Mkhabela et al., 2005). Elsewhere, studies found that the linear model to be ideal between winter wheat yield and NDVI in various regions (Ren et al., 2008; Lopresti et al., 2015; Franch et al., 2015).

3.3.6. Model validation

Statistical tests were performed to validate the performance of the model. The goodness of fit of the model and the percentage of variance explained by the model were assessed using the coefficient of determination (R^2). The significance of the model was tested by means of p-values. The Root Mean Squared Error (RMSE) was also included in the analysis. Diagnostic plots were constructed to compare the observed yield and the predicted yield. The residuals were plotted vs. the wheat yield,

this was necessary to check for linearity of the data and the presence or absence of inhomogeneity of variance (Larsen and McCleary, 1972). Additionally, a quantile-quantile (Q-Q) residual plot was used to assess how close the theoretical distribution is to the model distribution. A normal distribution is indicated by a strong linear pattern for the sample points, outliers can also be detected by visual inspection of the plot (Ben and Yohai, 2012). These validation methods differ from the widely used methods, in previous studies which mostly focus on the RMSE and comparing the correlation between observed yield and predicted yield. The validation techniques also aided in understanding the underlying trends in the data.

3.3.7. Model testing

The NDVI data for the years 2001/2002/2008/2011/2014 were used for model testing. These years were not used for model building, calibration, and model validation. The NDVI of these years was used to predict the expected wheat yield. The predicted yield was then subtracted from the observed yield and the percentage error was calculated for the observed yield. The standard error was used as a measure of the accuracy of the predicted yield where values close to zero indicate high accuracy. The year 2015 could not be used in the analysis due to severe drought in the non-irrigated wheat regions.

3.4. Results and discussion

3.4.1. Relationships between wheat yield and NDVI data

The best fitting model between wheat yield and NDVI was developed by using the Zadoks scale (Zadoks et al., 1974) to identify the critical growth stages of wheat. According to previous research carried out in other regions, the most critical growth stage for dryland wheat is anthesis (Aparicio et al., 2002; Moriondo et al., 2007; Lopresti et al., 2015). This stage was also highly correlated with the final wheat yield at Central Free State as with other regions. This time occurs approximately 30 days prior to harvest during the first week of November (Day of year 305 on regular years).

The linear relationship between the average yield and average NDVI are represented in Equation (3.5):

$$P(Y \mid x) = 12.1136x - 2.7307 \ \left(R^2 = 0.73,\ p = 0.00161\right). \quad (3.5)$$

In this study, the seasonal maximum NDVI was used to correlate with average wheat yields. The range of NDVI values for the model are between 0.32 and 0.49. These values fall within the threshold indicated by Ren et al., (2008) for winter wheat of 0.2 to 0.8. The observed yield was similar to the predicted yield (Table 4), the negative residuals indicated periods when the model underestimated yield and positive values indicated periods when the model overestimated yield. The model was calibrated using NDVI however, other parameters such as Growing Degree Days or Heat Units, soil conditions, weather conditions can also be considered in order to improve the accuracy of the model.

Table 4. The observed and predicted wheat yield derived using a simple linear regression model.

Year	Observed Yield (tons/ha)	Predicted Yield (tons/ha)	Residuals
2000	2.8971	2.2542	-0.64291
2003	1.0742	1.0736	-0.00063
2004	1.2697	1.3914	0.12172
2005	1.1170	1.6640	0.54699
2006	2.7885	2.5650	-0.22344
2007	2.8460	2.4662	-0.37975
2009	2.7575	3.1708	0.41329
2010	2.3952	2.2656	-0.12956
2012	2.2734	2.7527	0.47936
2013	2.6513	2.4662	-0.18504

3.4.2. Model validation

The regression models' predicted yield was compared to the observed yield from the ten-year winter wheat yield data (Figure 8). The p-value was 0.00161 ($p<0.05$) indicating a good significance and the R^2 explained 73% of the variability in wheat yield. These results are similar to those reported by Lopresti et al., (2015) of an R^2 of 0.75 for winter wheat yield in Northern Buenos Aires province, Argentina. The similarity of these results could be due to spatial location of Argentina and South Africa in the Southern Hemisphere. Periods for winter wheat production are similar for both countries because the seasonal cycles (winter is from June to September) coincide. However, Ren et al., (2008) observed an R^2 of 0.88 for Shandong (China) when relating the production of winter wheat with the accumulated MODIS derived NDVI.

The RMSE of the calibrated model was validated against the observed yield. An RMSE of 0.41 tons ha^{-1} results from using the least squares regression line to predict the wheat yield. Becker-Reshef et al., (2010) reported a similar RMSE of 0.44 tons ha^{-1} for Kansas using MODIS-NDVI for wheat forecasting. Moriondo et al., (2007) observed an RMSE of 0.44 tons ha^{-1} and 0.47 tons ha^{-1} respectively when using AVHRR-NDVI data to develop a wheat yield model for two Italian provinces.

Diagnostic plots were constructed to assess the fit of the model and whether the residuals are normally distributed. Residual plots (Figure 9A) were used to determine if the model was linear. Linear models have a random scatter of data points whereas non-linear models have a distinctive pattern (Larsen and McCleary, 1972). A random dispersal of the residuals was observed, which means that the linear model is an ideal fit between the wheat yield and NDVI. The Q-Q plot depicted in Figure 9B indicated that the residuals are homogeneous although small variations were present at the lower and upper tails of the plot. Periods of drought could induce such variations (outliers) and reduce the wheat yield since dryland wheat relies on residual soil moisture for growth. Overall, the residuals are normally distributed as they lie close to a straight line.

These diagnostic plots were necessary, as other studies have observed different relationships between vegetation indices and crop yields. Hayes and Decker (1998) observed a quadratic relationship between a satellite data variable, Vegetation Condition Index (VCI), Crop Moisture Index (CMI) and a climatological variable for predicting maize production. The R^2 value of the model was 0.73. Ma et al. (2001) reported a power function to be representative of the relationship between soybean yield and canopy reflectance measurements at different soil types. The R^2 value of the model was 0.80. Benedetti and Rossini (1993), Ren et al., (2008) and Lopresti et al., (2015) all observed a linear relationship between wheat yield and NDVI. However, Mkhabela et al., (2011) observed that a power function was representative of the relationship between NDVI and spring wheat at different environments. The differences in models for spring wheat and winter wheat could be induced by different weather conditions and irrigation as winter wheat in South Africa is not irrigated.

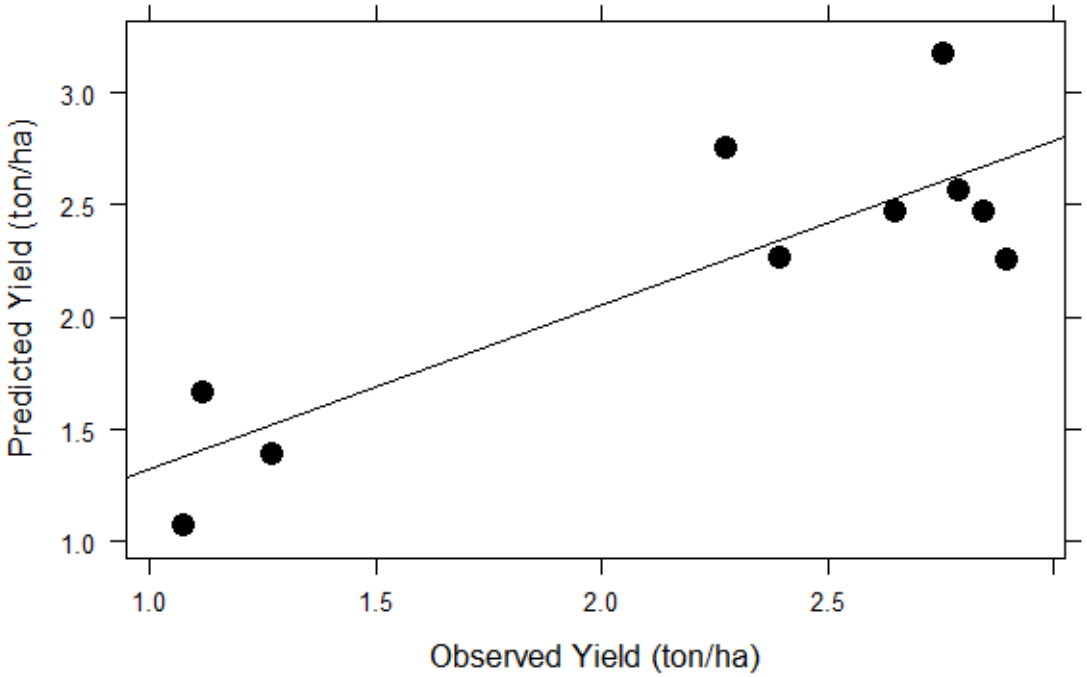

Figure 8. Central Free State predicted yield as a function of observed yield. Each point represents the observed and predicted yield for a particular year during the 10-year study period.

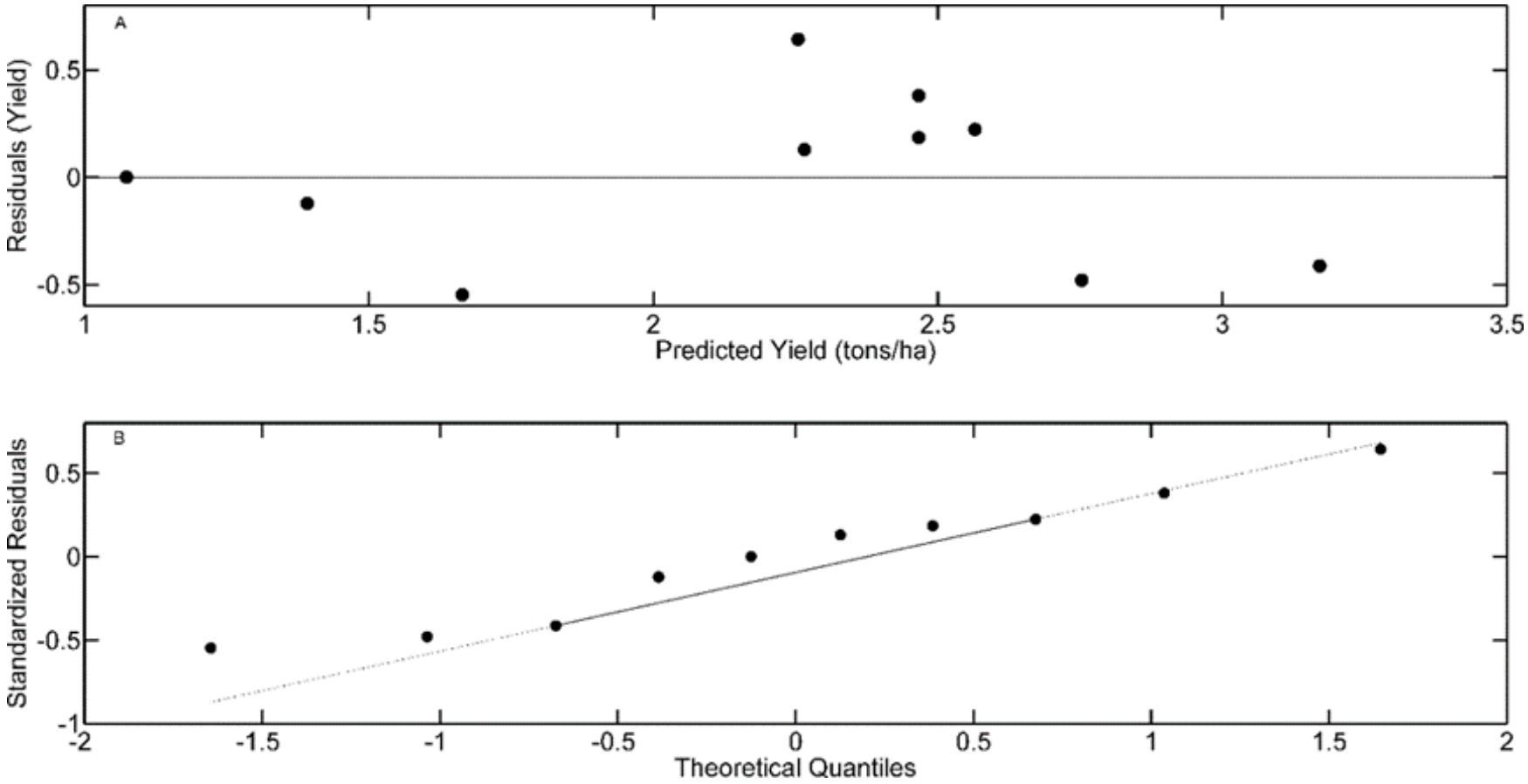

Figure 9. Model validation diagnostic plots. Panel (A) is the residual plot displaying randomly distributed residuals indicating that the linear model is the appropriate fit for the data. Panel (B) is the Q-Q plot; this clearly indicates that the residuals are normally distributed.

3.4.3. Model testing

The percentage errors in Table 5 indicate that the model slightly overestimated yield in 2002/8/11 because the values are above 10%. However, the model performed well in 2001 as the percentage errors are within the threshold of ±10%. The model predicted wheat yield well in 2014 since this year was not falling within the 2000-2013 period for which the model was calibrated. The standard errors were close to zero, which meant that the predicted yield has a reasonable level of accuracy and thus, the model was reliable.

Table 5. Model testing results for the observed and predicted yield.

Year	Observed Yield (O) ton/ha	Predicted Yield (P) ton/ha	Difference (O-P) ton/ha	%Diff for observed yield	Standard Error tons/ha
2001	2.7700	2.9627	-0.1927	-6.9567	0.0862
2002	1.9900	1.2300	0.7600	38.1910	0.3399
2008	1.2400	1.0003	0.2397	19.3306	0.1072
2011	1.7100	1.1730	0.5370	31.4035	0.2402
2014	2.4000	2.1300	0.2700	11.2500	0.1207

Throughout this study, MODIS data from an optical sensor was used but Synthetic Aperture Radar (SAR) data can also be used. The advantages of SAR are that it can operate during the day or night, and in rainy or cloudy conditions. However, SAR data requires complex processing, often specialized software such as the INAHOR (Oyoshi et al., 2015) and thus, was not a focus of this study. Data provided by satellites at a high resolution such as SPOT or RapidEye are better for small scale estimates of crop yield because many tiles are needed to cover a large area and thus costly.

3.5. Conclusion

The prospect of using MODIS-NDVI for winter wheat yield forecasts in the Central Free State production region was investigated using regression models. Findings suggest the best time to relate MODIS-NDVI to final wheat yields for this area is the period leading to 30 days before harvest (first week of November). This period coincides with the anthesis stage, and at this time, wheat yield is highly correlated to NDVI. The relationship between NDVI and wheat yield was significant with an R^2 value of 0.73, a p-value of 0.00161 and an RMSE of 0.41 tons ha^{-1}. Furthermore, diagnostic plots, model testing and validation provided evidence of the reasonable levels of model accuracy, model reliability, and a good fit. These techniques complement the widely used techniques of comparing the correlation between the observed yields and predicted yields and using the RMSE.

3.6. References

1. Aparicio, N., Villegas, D., Araus, J.L., Casadesus, J. and Royo, C., 2002. Relationship between growth traits and spectral vegetation indices in durum wheat. *Crop science*, 42(5), 1547-1555.
2. ARC, 2014. Guideline for the production of small grains in the summer rainfall areas. Free State.
3. Asner, G.P., Scurlock, J.M. and Hicke, J., 2003. Global synthesis of leaf area index observations: implications for ecological and remote sensing studies. *Global Ecology and Biogeography*, 12(3), 191-205.
4. Balkovič, J., van der Velde, M., Skalský, R., Xiong, W., Folberth, C., Khabarov, N., Smirnov, A., Mueller, N.D. and Obersteiner, M., 2014. Global wheat production potentials and management flexibility under the representative concentration pathways. *Global and Planetary Change*, 122, 107-121.
5. Bastiaanssen, W.G. and Ali, S., 2003. A new crop yield forecasting model based on satellite measurements applied across the Indus Basin, Pakistan. *Agriculture, Ecosystems & Environment*, 94(3), 321-340.
6. Becker-Reshef, I., Justice, C., Sullivan, M., Vermote, E., Tucker, C., Anyamba, A., Small, J., Pak, E., Masuoka, E., Schmaltz, J. and Hansen, M., 2010. Monitoring global croplands with coarse resolution earth observations: The Global Agriculture Monitoring (GLAM) project. *Remote Sensing*, 2(6), 1589-1609.
7. Ben, M.G. and Yohai, V.J., 2012. Quantile–quantile plot for deviance residuals in the generalized linear model. *Journal of Computer and Graph Statistics*, 13(1), 36-47.
8. Benedetti, R. and Rossini, P., 1993. On the use of NDVI profiles as a tool for agricultural statistics: the case study of wheat yield estimate and forecast in Emilia Romagna. *Remote Sensing of Environment*, 45(3), 311-326.
9. Breitenbach, M.C. and Fényes, T.I., 2000. Maize and wheat production trends in South Africa in a deregulated environment. *Agrekon*, 39, 292-312.
10. Byerlee, D., Jayne, T.S. and Myers, R.J., 2006. Managing food price risks and instability in a liberalizing market environment: Overview and policy options. *Food Policy*, 31(4), 275-287.
11. Carlson, T.N. and Ripley, D.A., 1997. On the relation between NDVI, fractional vegetation cover, and leaf area index. *Remote Sensing of Environment*, 62(3), 241-252.
12. Chen, P.Y., Fedosejevs, G., Tiscareno-Lopez, M. and Arnold, J.G., 2006. Assessment of MODIS-EVI, MODIS-NDVI and VEGETATION-NDVI composite data using agricultural measurements: an example at corn fields in western Mexico. *Environmental Monitoring and Assessment*, 119(1-3), 69-82.
13. Dube, E., Mare-Patose, R., Kilian, W., Barnard, A. and Tsilo, T.J., 2015. Identifying high-yielding dryland wheat cultivars for the summer rainfall area of South Africa. *South African Journal of Plant and Soil*, 1-5.

14. Dwyer, J. and Schmidt, G., 2006. The MODIS reprojection tool. In: Qu, J.J., Gao, W., Kafatos, M., Murphy, R.E., Salomonson, V.V. (Eds.), Earth Science Satellite Remote Sensing. Springer Berlin Heidelberg, Berlin Heidelberg, 162–177.
15. Franch, B., Vermote, E.F., Becker-Reshef, I., Claverie, M., Huang, J., Zhang, J., Justice, C. and Sobrino, J.A., 2015. Improving the timeliness of winter wheat production forecast in the United States of America, Ukraine and China using MODIS data and NCAR growing degree day information. *Remote Sensing of Environment*, 161, 131-148
16. Frost, C., Thiebaut, N. and Newby, T., 2013. Evaluating Terra MODIS Satellite Sensor Data Products for Maize Yield Estimation in South Africa. *South African Journal of Geomatics*, 2, 106-119.
17. Gallo, K., Lei, J., Reed, B., Eidenshink, J. and Dwyer, J., 2005. Multi-platform comparisons of MODIS and AVHRR normalized difference vegetation index data. *Remote Sensing of Environment*, 99(3), 221-231.
18. Giunta, F., Motzo, R. and Deidda, M., 1993. Effect of drought on yield and yield components of durum wheat and triticale in a Mediterranean environment. *Field Crops Research*, 33(4), 399-409.
19. Goward, S.N., Markham, B., Dye, D.G., Dulaney, W. and Yang, J., 1991. Normalized difference vegetation index measurements from the Advanced Very High Resolution Radiometer. *Remote Sensing of Environment*, 35(2-3), 257-277.
20. Hammer, G.L., Hansen, J.W., Phillips, J.G., Mjelde, J.W., Hill, H., Love, A. and Potgieter, A., 2001. Advances in application of climate prediction in agriculture. *Agricultural Systems*, 70(2), 515-553.
21. Hayes, M.J. and Decker, W.L., 1998. Using satellite and real-time weather data to predict maize production. *International Journal of Biometeorology*, 42(1), 10-15.
22. Hensley, M., Le Roux, P., Du Preez, C., Van Huyssteen, C., Kotze, E. and Van Rensburg, L., 2006. Soils: the Free State's agricultural base. *South African Geographical Journal*, 88(1), 11-21.
23. Huete, A., Didan, K., Miura, T., Rodriguez, E.P., Gao, X. and Ferreira, L.G., 2002. Overview of the radiometric and biophysical performance of the MODIS vegetation indices. *Remote Sensing of Environment*, 83(1), 195-213.
24. Justice, C.O., Vermote, E., Townshend, J.R., Defries, R., Roy D.P., Hall, D.K., Salomonson, V.V., Privette, J.L., Riggs, G., Strahler, A., Lucht, W., Myneni, R. B., Knyazikhin, Y., Running, S.W., Nemani, R.R., Wan, Z., Huete, A.R., van Leeuwen, W., Wolfe, R.E., Giglio, L., Muller, J., Lewis, L. and Barnsley M.J., 1998. The Moderate Resolution Imaging Spectroradiometer (MODIS): Land remote sensing for global change research. *IEEE Transactions on Geoscience and Remote Sensing,* 36(4), 1228-1249.

25. Kim, S.R., Prasad, A.K., El-Askary, H., Lee W.K., Kwak, D.K. and Lee, S.H., 2014. Application of the Savitzky-Golay filter to land cover classification using temporal MODIS vegetation indices. *Photogrammetry, Engineering & Remote Sensing*, 80(7), 675-685.
26. Larsen, W.A. and McCleary, S.J., 1972. The use of partial residual plots in regression analysis. *Technometrics*, 14(3), 781-790.
27. Lopresti, M.F., Di Bella, C.M. and Degioanni, A.J., 2015. Relationship between MODIS-NDVI data and wheat yield: A case study in Northern Buenos Aires province, Argentina. *Information Processing in Agriculture*, 2(2), 73-84.
28. Ma, B.L., Dwyer, L.M., Costa, C., Cober, E.R. and Morrison, M.J., 2001. Early prediction of soybean yield from canopy reflectance measurements. *Agronomy Journal*. 93(6), 1227-1234.
29. Mkhabela, M.S., Mkhabela, M.S. and Mashinini, N.N., 2005. Early maize yield forecasting in the four agro-ecological regions of Swaziland using NDVI data derived from NOAA's-AVHRR. *Agricultural and Forest Meteorology*, 129(1), 1-9.
30. Mkhabela, M.S., Bullock, P., Raj, S., Wang, S. and Yang, Y., 2011. Crop yield forecasting on the Canadian Prairies using MODIS NDVI data. *Agricultural and Forest Meteorology*, 151(3), 385-393.
31. Moriondo, M., Maselli, F. and Bindi, M., 2007. A simple model of regional wheat yield based on NDVI data. *European Journal of Agronomy*, 26, 266–274.
32. Mutanga, S., van Schoor, C., Olorunju, P.L., Gonah, T. and Ramoelo, A., 2013. Determining the Best Optimum Time for Predicting Sugarcane Yield Using Hyper-Temporal Satellite Imagery. *Advances in Remote Sensing*, 2(03), 269-275.
33. Nuarsa, I.W., Nishio, F. and Hongo, C., 2011. Rice yield estimation using Landsat ETM+ data and field observation. *Journal of Agricultural Science*, 4(3), 45-56.
34. Ortiz, R., Sayre, K.D., Govaerts, B., Gupta, R., Subbarao, G.V., Ban, T., Hodson, D., Dixon, J.M., Ortiz-Monasterio, J.I. and Reynolds, M., 2008. Climate change: Can wheat beat the heat?. *Agriculture, Ecosystems & Environment*, 126(1), 46-58.
35. Oyoshi, K., Tomiyama, N., Okumura, T. and Sobue, S., 2015. Mapping rice-planted areas using time-series synthetic aperture radar data for the Asia-RiCE activity. *Paddy Water Environment,* 14(4), 463-472.
36. Parry, M.L., Rosenzweig, C., Iglesias, A., Livermore, M. and Fischer, G., 2004. Effects of climate change on global food production under SRES emissions and socio-economic scenarios. *Global Environmental Change*, 14(1), 53-67.
37. Reed, B.C., Brown, J.F., Van der Zee, D., Loveland, T.R., Merchant, J.W. and Ohlen, D.O., 1994. Measuring phenological variability from satellite imagery. *Journal of Vegetation Science*, 5(5), 703-714.
38. Ren, J., Chen, Z., Zhou, Q. and Tang, H., 2008. Regional yield estimation for winter wheat with MODIS-NDVI data in Shandong, China. *International Journal of Applied Earth Observation and Geoinformation*, 10(4), 403-413.

39. Royo, C., Voltas, J. and Romagosa, I., 1999. Remobilization of pre-anthesis assimilates to the grain for grain only and dual-purpose (forage and grain) triticale. *Agronomy Journal*, 91(2), 312-316.
40. Salomonson, V.V., Barnes, W. L., Maymon, P. W., Montgomery, H. E., Ostrow, H., 1989. MODIS: advanced facility instrument for studies of the earth as a system. *IEEE Transactions on Geoscience and Remote Sensing*, 27(2), 145-153.
41. Savitzky, A. and Golay, M.J., 1964. Smoothing and differentiation of data by simplified least squares procedures. *Analytical Chemistry*, 36(8), 1627-1639.
42. Singh, R., Semwal, D., Rai, A. and Chikara, R.S., 2002. Small area estimation of crop yield using remote sensing satellite data. *International Journal of Remote Sensing*, 25, 49-56.
43. Tucker, C.J., 1979. Red and photographic infrared linear combinations for monitoring vegetation. *Remote Sensing of Environment*, 8(2), 127-150.
44. Unganai, L.S. and Kogan, F.N., 1998. Drought Monitoring and Corn Yield Estimation in Southern Africa from AVHRR Data. *Remote Sensing of Environment*, 63, 219-232.
45. Vermote, E.F., El Saleous, N., Justice, C.O., Kaufman, Y.J., Privette, J.L., Remer, L., Roger, J.C. and Tanre, D., 1997. Atmospheric correction of visible to middle-infrared EOS-MODIS data over land surfaces: Background, operational algorithm and validation. *Journal of Geophysical Research: Atmospheres*, 102 (D14), 17131-17141.
46. Vermote, E.F., El Saleous, N.Z. and Justice, C.O., 2002. Atmospheric correction of MODIS data in the visible to middle infrared: first results. *Remote Sensing of Environment*, 83(1), 97-111.
47. Walthall, C.L., Norman, J.M., Welles, J.M., Campbell, G. and Blad, B.L., 1985. Simple equation to approximate the bidirectional reflectance from vegetative canopies and bare soil surfaces. *Applied Optics*, 24(3), 383-387.
48. Wang, Z., Liu, C. and Huete, A., 2002. From AVHRR-NDVI to MODIS-EVI: Advances in vegetation index research. *Acta Ecologica Sinica*, 23(5), 979-987.
49. Wheeler, T.R., Hong, T.D., Ellis, R.H., Batts, G.R., Morison, J.I.L. and Hadley, P., 1996. The duration and rate of grain growth, and harvest index, of wheat (Triticum aestivum L.) in response to temperature and CO2. *Journal of Experimental Botany*, 47(5), 623-630.
50. Wolfe, R.E., Nishihama, M., Fleig, A.J., Kuyper, J.A., Roy, D.P., Storey, J.C. and Patt, F.S., 2002. Achieving sub-pixel geolocation accuracy in support of MODIS land science. *Remote Sensing of Environment*, 83(1), 31-49.
51. Wu, C., Niu, Z. and Gao, S., 2010. Gross primary production estimation from MODIS data with vegetation index and photosynthetically active radiation in maize. *Journal of Geophysical Research: Atmospheres*, 115(D12), 1-11.
52. Yang, C., Everitt, J.H. and Bradford, J.M., 2006. Comparison of QuickBird satellite imagery and airborne imagery for mapping grain sorghum yield patterns. *Precision Agriculture*, 7(1), 33-44.

53. Zadoks, J.C., Chang, T.T. and Konzak, C.F., 1974. A decimal code for the growth stages of cereals. *Weed research*, 14(6), 415-421.

Chapter 4

Evaluating the influence of agrometeorological parameters for winter wheat yield forecasting

Based on: Mashaba, Z., Chirima, G., Botai, J. and Munghemezulu, C., 2017. Evaluating the influence of agrometeorological parameters for winter wheat yield forecasting. *South African Geographical Journal.* (Submitted, manuscript ID: RSAG-2017-0021)

Abstract

Crop yield forecasting is a crucial process for ensuring food security in a country. However, current crop yield prediction techniques used in South Africa rely on manual field surveys, which are costly and not timely for decision making. Therefore, there is a need for using remotely sensed data, which is freely available for crop yield forecasting. Ten years of wheat yield data, NDVI and agrometeorological data such as: soil moisture, evapotranspiration and surface temperature were used to calibrate and validate a multi-linear regression forecasting model. The model was tested using five years of independent data. The importance of each agrometeorological parameter in wheat yield forecasting was investigated using a correlation matrix. The calibrated model had a coefficient of determination (R^2) of 0.82 and a p-value of 0.0444. The Root Mean Square Error (RMSE) was close to zero indicating a good level of accuracy. Computed Mean Bias Errors (MBE) gave an indication that the predicted yield was similar to the observed yield. Percentage relative errors were ±10% for the model testing data with exception to 2010 and 2013, which indicated a reasonable level of accuracy. Parameters identified as important for wheat yield forecasting using a correlation matrix were the NDVI (r=0.88) and evapotranspiration (r=0.58). This study proved that remote sensing can be used at high levels of accuracy for forecasting wheat yield to aid timely decision making regarding imports and exports.

Keywords: wheat yield, agrometeorological parameter, food security, remote sensing

4.1. Introduction

Global food security is threatened by a declining investment in agricultural research, variable water resources for irrigation, and a lack of development of rural infrastructure (Rosegrant and Cline, 2003). Additionally, environmental factors in semi-arid regions such an increasing temperature and a decrease in precipitation have the potential of reducing the yields of essential crops such as maize, wheat, and rice (Lobell et al., 2008). In South Africa, wheat is the second most important component forming part of the staple diet after maize (Breitenbach and Fenyes, 2000). Therefore, accurate predictions of wheat yields early in the season are vital for food security. In this research, different meteorological factors influencing wheat yield are integrated for the development of a wheat yield forecasting model for the Central Free State region.

Several studies have been done using statistical models based on agrometeorological indices such as: growing degree days, temperature difference, photothermal units, heliothermal units, vapour pressure deficit, potential evapotranspiration, and relative deviation for predicting wheat yield (Bazgeer et al. 2007; Esfandiary et al., 2009; Kingra and Prabhjyot-Kaur, 2013). However, the combination of NDVI with other parameters such as surface temperature, precipitation, and soil moisture is not well studied for estimating crop yields (Bakker et al., 2005; Prasad et al., 2006; Balaghi et al., 2008). The addition of such parameters in crop yield forecasting models incorporates information about the environmental conditions, which influence crop growth. However, most studies focus on the NDVI as a primary predictor of crop yield (Prasad et al., 2006).

In South Africa, there is a lack of studies using remote sensing for crop yield predictions. However, yield predictions rely on farmer interviews, manual field surveys and aerial surveys. These methods are not timely for decision making and are costly. The use of low cost UAVs can overcome the challenges of timeliness and consistency on a farm scale or field trails, but not on a regional scale as compared to satellite remote sensing imagery (Grenzdörffer et al., 2008; Berni et al., 2009). Establishing a method based on remotely sensed data such as the one developed in this research is of vital importance.

4.2. Background

Crop models are a simplified representation of a crop used to understand crop growth and the growth responses to the environment (Miglietta and Bindi, 1993). The development stages on research regarding yield estimation research using crop simulation models are summarized in Sun (2000): prior to the 1940s, quantitative analysis through comparison between meteorological conditions and crop yield were used. In the 1950s, regression models (empirical statistical approach) between crop yield and weather conditions were developed. In the 1960s, advances in the development and application of computers led to researchers developing different crop simulation models. The two commonly used approaches for estimating crop yields integrating agrometeorological variables are reviewed. The empirical statistical approach is adopted in the current research.

4.2.1. Empirical statistical approaches

Empirical statistical approaches characterize the relationship between crop yield and meteorological variables using regression relationships. The accuracy of the results obtained from statistical models is dependent on the representativeness of the meteorological input data, variables used for model calibration and the accuracy of the data (Baier, 1979; Nonhebel, 1994). Statistical models are particularly useful for large area crop estimates and are often not possible to extrapolate to other areas (Liu, 2009). The cause and effect relationships are not defined by statistical models but they provide a basis for understanding the past, present and future crop yield expected (Baier, 1979).

The availability of remotely sensed data and field observed data has made it possible to have studies characterizing the relationship between agrometeorological data and yields (Ceglar et al., 2016). Balaghi et al., (2008) developed an ordinary least squares model to predict the grain yield of wheat for Morocco by making use of NDVI, rainfall and temperature data. The model forecasting ability was better at a provincial level as compared to a national level. Prasad et al., (2006) used the Quasi-Newton method to predict maize and soybean yields by incorporating NDVI, soil moisture, surface temperature and rainfall data for Iowa state in the United States. In the study, the

Quasi-Newton method minimized inconsistencies in yield prediction, which improved the R^2 values. Bakker et al., (2005) investigated the factors, which contribute to the variability and trends in wheat yields across Europe by using climate, soil and economic variables. In the study, it was reported that the Nomenclature of Territorial Units for Statistics (NUTS3) level climate and soil conditions where explanatory variables for the variability of wheat yields in Europe.

Different statistical techniques have been used for predicting crop yields. Ji et al., (2007) used artificial neural networks in predicting rice yield. Wendroth et al., (2003) used autoregressive state-space models for predicting barley yield. Foody (2003) demonstrated how geographical weighting can improve regression models for crop yield using the NDVI and rainfall. Ma et al., (2001) used an exponential model to predict soybean yields. Hansen et al., (2002) used least squares regression model for wheat and barley yield prediction. The commonly used statistical method of crop yield forecasting are regression relationships combining NDVI and crop yields (Prasad et al., 2007).

4.2.2. Crop growth simulation models

Crop growth simulation models simulate the growth, development and yield of a crop using soil, weather, crop varieties and management practices data as input (Jones et al., 2003). The meteorological parameters used in these type of models are: the solar radiation, temperature, humidity and precipitation (Baier, 1979). There is a challenge of obtaining these weather data for model calibration especially solar radiation data because it is usually not measured at experimental sites. The common practice is to derive the solar radiation from sunshine hours if the Amström coefficients are known (Hoogenboom, 2000). Crop models are point or site specific and are often not applied at a national scale (Liu, 2009).

Different crop models simulation models which make use of agrometeorological parameters for yield estimations are used in agriculture. The CropSyst crop model has proven capabilities in the estimation of rice, alafa and water yam (Confalonieri and Bechini, 2004; Confalonieri and Bocchi, 2005; Macros et al., 2011). The WOFOST

crop model has been applied modelling sunflower growth and compared to the AquaCrop and CropSyst crop simulation models (Todorovic et al., 2009). The EPIC crop model has been applied in simulating cotton yield (Ko et al., 2009). Farre et al., (2002) applied APSIM crop model for simulating canola yield.

This research focuses specifically on forecasting winter wheat yield. Palosuo et al., (2011) compared the performance of eight crop simulation models in estimating winter wheat yield. In the study it was observed that DAISY and DSSAT were the most accurate in predicting wheat yields. The CropSyst crop simulation model underestimated the yield. The HERMES, STICS, FASSET, APES and WOFOST models overestimated the yield. Recently, Castañeda-Vera et al., (2015) compared the performance of AquaCrop, CERES-Wheat, CropSyst and WOFOST crop simulation models for simulating winter wheat yield. In the study, it was observed that CERES-Wheat and CropSyst are superior in simulating winter wheat yield at field levels in semi-arid conditions. The WOFOST model was found to be best applied in situations where data on soil is limited and the AquaCrop model is best applied when water availability is not limited.

4.3. Data and methods

4.3.1. Study area

The Free State province contributes 41% of the maize production in South Africa and 30% of the wheat (NDA, 2005; SAGL, 2013). Temperatures of Free State can be low as -5 °C in winter and high as 35 °C in summer. The average rainfall is 600 mm to 750 mm in the east and less than 300 mm in the west (DRDLR, 2013). There are four dryland wheat production regions in Free State divided into: Central Free State, North Western Free State, South Western Free State, and Eastern Free State (ARC, 2014). The 3803 wheat fields of Central Free State considered in the study are represented as points in Figure 10.

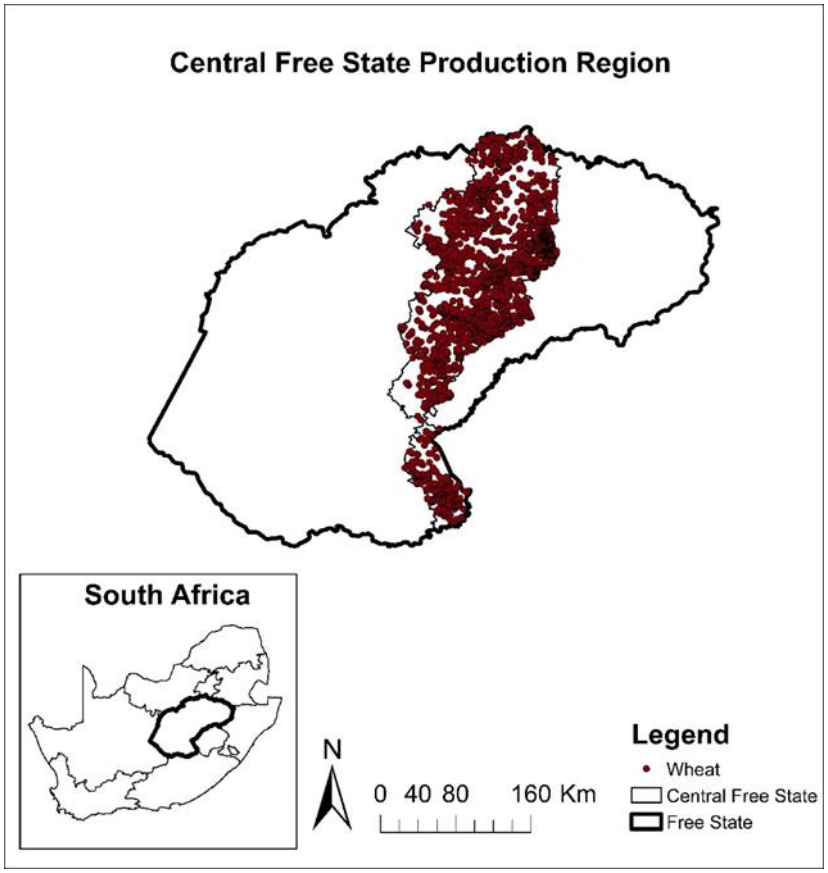

Figure 10. The wheat farms within Central Free State depicted as points.

4.3.2. Data

Wheat yield data for the period of 2000-2014 was used in the study. This data was related to surface parameters important for dryland winter wheat growth such as: NDVI, soil moisture, evapotranspiration and surface temperature depicted in Figure 11. The surface temperature increased over the years as compared to the other surface parameters which showed slight fluctuations. These parameters were derived from monthly satellite imagery described in section 4.3.4 - 4.3.7 instead of in situ measurements because meteorological stations are not well distributed throughout the study area. The period selected for modelling was November since wheat harvesting takes place in December.

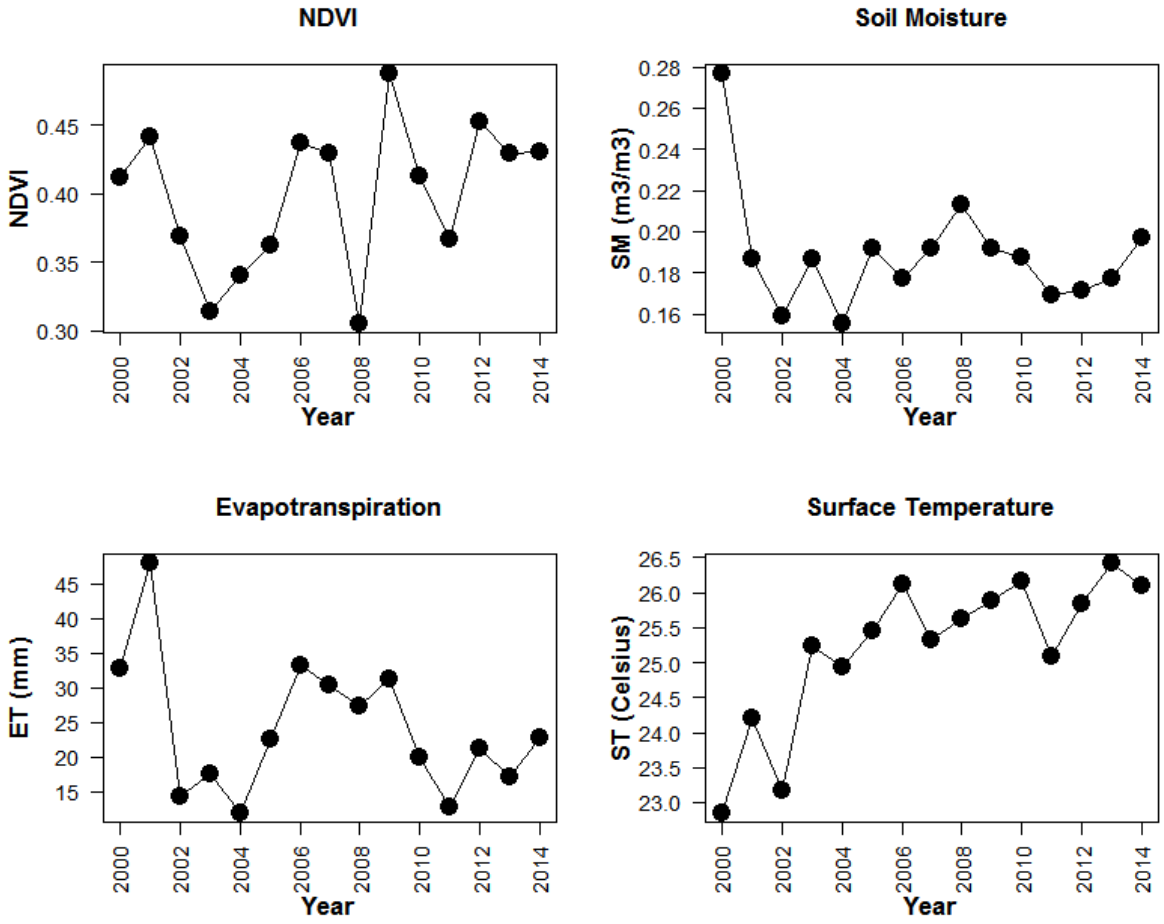

Figure 11. Annual variation of the parameters important for winter wheat growth. The mean of the 3803 wheat fields of Central Free State are depicted.

4.3.3. Wheat yield data

The wheat yield data (Figure 12) was obtained from the Agricultural Research Council Small Grain Institute (ARC-SGI). The wheat production sites part of the National Wheat Cultivar Evaluation Programme (NWCEP) were used to obtain wheat yield data. Planting takes place from the first week of July for the late wheat plantings (ARC, 2014). The wheat farm boundaries were obtained from the ARC which collaborates with Geo Terra Image (GTI) and Spatial Business Intelligence (SIQ).

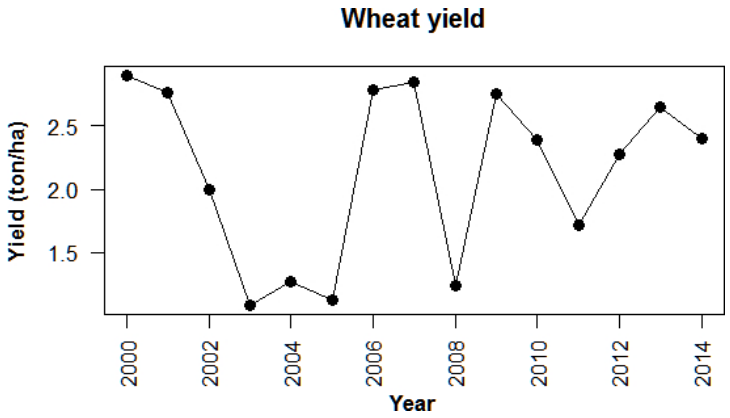

Figure 12. Wheat yield data for the period of 2000-2014 for Central Free State.

4.3.4. Normalized Difference Vegetation Index

The MOD13A3 MODIS NDVI monthly images at a 1 km spatial resolution were obtained from the National Aeronautical Space Agency (NASA) Earth Observing System (EOS). The NDVI images were reprojected from Sinusoidal to Geographic coordinates using the MODIS Reprojection Tool (MRT). The two tiles h20v11 and h20v12 were mosaicked and rescaled to range between -1 and 1. The NDVI values were extracted per pixel for wheat fields depicted in Figure 10 for each year. The same procedure was followed for extracting the soil moisture, evapotranspiration and surface temperature values.

4.3.5. Soil moisture

The soil moisture content for a depth of 0-10 cm underground was obtained from NASA Earth data. The monthly data are collected at a spatial resolution of 1° with units of $m^3.m^{-3}$. The soil moisture content is derived using the Global Land Data Assimilation System (GLDAS) which integrates satellite data from the Advanced Microwave Scanning Radiometer (AMSR) and ground based data to generate land parameters (Rodell et al., 2004).

4.3.6. Evapotranspiration

The monthly MOD16 evapotranspiration product of a spatial resolution of 1 km was obtained from the University of Montana's Numerical Terradynamic Simulation group. The evapotranspiration is derived using the algorithm detailed in Mu et al., (2011). MODIS Aqua tiles of h20v11 and h20v12 were mosaicked and projected to geographic co-ordinates using the MRT before extracting the evapotranspiration values.

4.3.7. Surface temperature

The monthly surface skin temperature was obtained from NASA Earth data. The product has a spatial resolution of 0.5×0.667° and is derived using the MERRA model which assimilates satellite data from the National Oceanic and Atmospheric Administration (NOAA), MODIS Aqua, Geostationary Operational Environmental Satellite system (GEOS) etc. (Rienecker et al., 2011). Surface skin temperature was in units of Kelvin but converted to degrees Celsius before extraction of the values.

4.3.8. Statistical Analysis

The meteorological parameters were related to wheat yields by means of a multiple linear regression model depicted in Equation (4.1) for the years 2000-2013 (excluding 2001, 2002, 2008, 2011, and 2014). The p-value was used to assess the significance of the model and the coefficient for determination (R^2) was used to test the goodness of fit of the calibrated model. The model was validated by means of the Root Mean Square Error (RMSE) in Equation (4.2) and the Mean Bias Error (MBE) in Equation (4.3). Additionally, the observed yield was plotted against the predicted yield. Model testing was done using independent data for 2001, 2002, 2008, 2011, and 2014 not used for model calibration and validation. The period of 2015 was not included in the analysis due to drought conditions in summer rainfall areas of Free State. Statistical test used to test the calibrated model were the RMSE in Equation (4.2) and the percentage relative error (RE) in Equation (4.4). The following equations were used for data analysis:

$$Yield = c_1 \times NDVI + c_2 \times SM \times c_3 \times ET + c_4 \times ST + c_5 + \varepsilon, \quad (4.1)$$

$$RMSE = \sqrt{\frac{\Sigma(O-P)^2}{N}}, \quad (4.2)$$

$$MBE = \frac{1}{N}\Sigma(O-P), \quad (4.3)$$

$$\%RE = \frac{O-P}{O} \times 100, \quad (4.4)$$

where, c_x are the respective coefficients, ε is the error term which indicates factors not accounted for in the model, *N* is the number of observations, *O* is the observed yield, and *P* is the predicted yield.

4.4. Results and discussion

4.4.1. Model development

The calibrated wheat forecasting model incorporating NDVI, soil moisture, evapotranspiration and surface temperature related well with the observed yield. The model explained 82% of the variability and a p-value of 0.0444 (<0.05) which meant that the model was statistically significant. The results are similar to those observed by Balaghi et al., (2008) of R^2 values of 0.64 to 0.98 for wheat grain yields in Morroco. In that study, NDVI, rainfall, and temperature were used as predictors of wheat yield. Prasad et al., (2006) observed R^2 values of 0.78 for maize and 0.86 for soybean. The study combined NDVI, precipitation, temperature, and soil moisture for crop yield predictions in Iowa (United States). The model calibrated in the current research is given in Equation (4.5):

$$\begin{aligned} Yield = {} & 10.9483 \times NDVI + 6.3938 \times SM + 0.0075 \times \\ & ET + 0.02133 \times ST - 4.1967 \\ & R^2 = 0.8156,\ p = 0.0444. \end{aligned} \quad (4.5)$$

The observed yield compared well with predicted yield, the results are depicted in Figure 13 and Table 6. The RMSE was close to zero which indicated that the predicted yield was similar to the observed yield and there was low level of inaccuracy. This

meant that the parameters selected for model calibration were descriptive of wheat yield. The MBE gave an indication whether the model underestimated (negative values) or overestimated yield (positive values). These differences in yield could be induced by factors such as: pests, changes in planting date, weeds, and pathogens (Oerke, 2006; Pathak et al., 2003) which affect non-irrigated wheat yield not accounted for in the model. The final wheat yield can also be affected by sudden meteorological event which occurring before harvest (Becker-Reshef et al., 2010). In this model, changes in the soil moisture, evapotranspiration and surface temperature can cause yield variabilities because forecasts are done a month before harvesting which takes place in December.

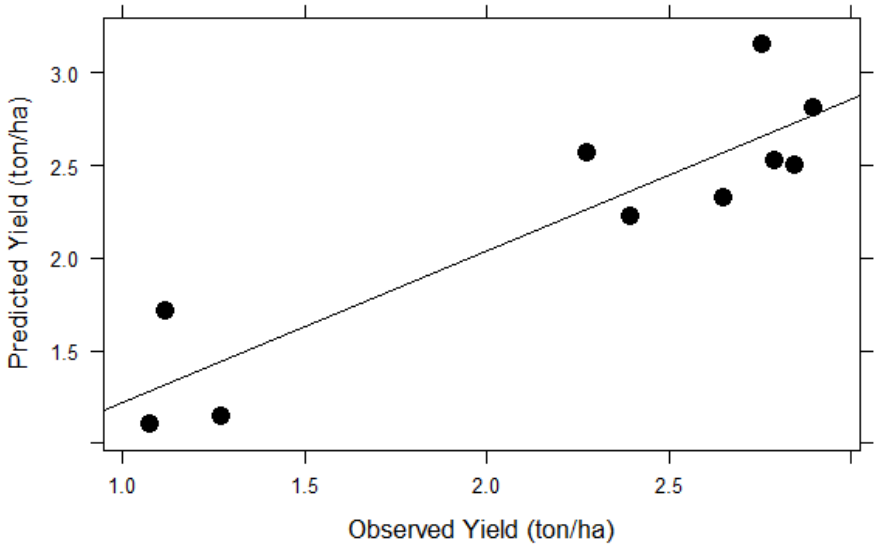

Figure 13. The predicted wheat yield related to the observed yield. Each point represents a year for the period of 2000-2009.

Table 6. The observed and predicted wheat yield derived using an agrometeorological parameter based multiple linear regression model and statistical tests to validate the model.

Years	Observed Yield (ton/ha)	Predicted yield (ton/ha)	RMSE	MBE
2000	2.8971	2.8090	0.0279	0.0088
2003	1.0742	1.1056	0.0099	-0.0031
2004	1.2697	1.1455	0.0393	0.0124
2005	1.1170	1.7130	0.1885	-0.0596
2006	2.7885	2.5298	0.0818	0.0259
2007	2.8459	2.4975	0.1102	0.0348
2009	2.7575	3.1514	0.1246	-0.0394
2010	2.3952	2.2264	0.0534	0.0169
2012	2.2734	2.5657	0.0924	-0.0292
2013	2.6513	2.3259	0.1029	0.0325

4.4.2. Model Testing

The calibrated model was tested using data from 2001, 2002, 2008, 2011, and 2014, which was not used to develop the model. Model testing assesses the validity of a regression model and provides statistical evidence on whether the model estimates the yield accurately. The model testing results are depicted in Table 5 indicating how the predicted yield varied from the observed yield. The percentage relative errors were close to ±10% for the years 2001, 2008, 2011, and 2014, which is statistically significant. However, variations were observed for 2002, with relative errors greater than 10%. The RMSE was close to zero, which indicated that the predicted yield was similar to the observed yield and the level of accuracy was reasonable.

Table 5. Model testing results for the agrometeorological parameter based model.

Year	Observed Yield (ton/ha)	Predicted Yield (ton/ha)	%Relative error	RMSE
2001	2.7700	2.7097	2.1754	0.0121
2002	1.9900	1.4585	26.7063	0.1063
2008	1.2400	1.2622	-1.7935	0.0044
2011	1.7100	1.5332	10.3405	0.0354
2014	2.4000	2.5095	-4.5625	0.0219

The consistency at which the yield estimates are derived from field surveys can affect the predicted yield, thereby, causing variations in the errors. Changes in agrometeorological parameters within the season can also cause yield variations. The model developed in the current study can be updated with the data used for model testing because the data has an acceptable level of accuracy for future wheat forecasting. This is recommended because agrometeorological parameters change every season and forecasts are more accurate if the model is updated continuously.

4.4.3. The relative influence of the selected agrometeorological parameters on wheat yield

The importance of each of the agrometeorological parameters used to develop the yield forecasting model was investigated. A correlation matrix was derived to assess the strength of the relationships amongst the parameters with relation to wheat yield, the resulting matrix depicted in Figure 14. The NDVI is strongly related to wheat yield, with correlation value of 0.88 followed by the evapotranspiration, which had a correlation value of 0.58. These results are expected because the wheat in Central Free State is non-irrigated and the area experiences summer rainfall. This means that the evapotranspiration is an important component, typical of other semi-arid areas as determined by Moussa et al., (2007). In terms of NDVI, many studies have proven that the NDVI is related to wheat yield (Benedetti and Rossini, 1993; Ma et al., 2001; Ren et al., 2008; Lopresti et al., 2015). Though the soil moisture and surface temperature

are not directly related to wheat yield, these variables can be used to improve NDVI based models, but not as sole predictors of wheat yield.

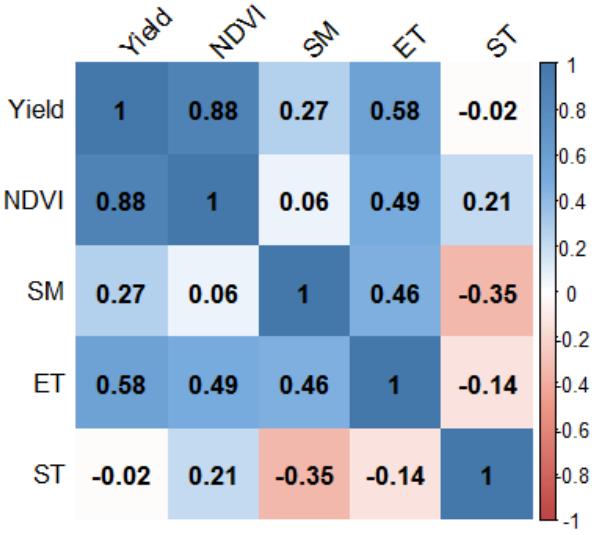

Figure 14. Correlation matrix of the agrometeorological factors influencing wheat yield.

4.5. Conclusion

The potential of using an agrometeorological parameter based model for wheat yield forecasting in Central Free State was investigated in this research. The importance of selected agrometeorological parameters in wheat forecasting was also investigated. The NDVI was related to satellite derived soil moisture, evapotranspiration and surface temperature through a multi-linear regression model for wheat yield forecasting. The calibrated model explained 82% of the variability and a p-value of 0.0444 (<0.05) which meant that the model was statistically significant. Differences between the observed yield and the predicted yield were attributed to factors not accounted for in the model. Model testing with independent data confirmed that the model had reasonable level of accuracy. The parameters important for wheat yield modelling in the Central Free State were the NDVI and the evapotranspiration. This study proved that remote sensing can be used for wheat yield modelling to overcome the problems of timeliness and cost of manual surveys for yield predictions in South Africa. The incorporation of agrometeorological parameters in the wheat yield model increased the predictive capacity of the model.

4.6. References

1. ARC, 2014. Guideline for the production of small grains in the summer rainfall areas. Free State.
2. Baier, W., 1979. Note on the terminology of crop—weather models. *Agricultural Meteorology*, 20(2), 137-145.
3. Bakker, M.M., Govers, G., Ewert, F., Rounsevell, M. and Jones, R., 2005. Variability in regional wheat yields as a function of climate, soil and economic variables: assessing the risk of confounding. *Agriculture, Ecosystems & Environment*, 110(3), 195-209.
4. Balaghi, R., Tychon, B., Eerens, H. and Jlibene, M., 2008. Empirical regression models using NDVI, rainfall and temperature data for the early prediction of wheat grain yields in Morocco. *International Journal of Applied Earth Observation and Geoinformation*, 10(4), 438-452.
5. Bazgeer, S., Kamali, G. and Mortazavi, A., 2007. Wheat yield prediction through agrometeorological indices for Hamedan, Iran. *Baiban*, 12, 33-38.
6. Becker-Reshef, I., Vermote, E., Lindeman, M. and Justice, C., 2010. A generalized regression-based model for forecasting winter wheat yields in Kansas and Ukraine using MODIS data. *Remote Sensing of Environment*, 114(6), 1312–1323.
7. Benedetti, R. and Rossini, P., 1993. On the use of NDVI profiles as a tool for agricultural statistics: the case study of wheat yield estimate and forecast in Emilia Romagna. *Remote Sensing of Environment*, 45 (3), 311-326.
8. Berni, J.A.J., Zarco-Tejada, P.J., Suárez, L., González-Dugo, V. and Fereres, E., 2009. Remote sensing of vegetation from UAV platforms using lightweight multispectral and thermal imaging sensors. *International Archives of Photogrammetry Remote Sensing and Spatial Information Science*, *38*(6).
9. Breitenbach M.C. and Fenyes, T.I., 2000. Maize and wheat production trends in South Africa in a deregulated environment. *Agrekon*, 39(3), 292-312.
10. Castañeda-Vera, A., Leffelaar, P.A., Álvaro-Fuentes, J., Cantero-Martínez, C. and Mínguez, M.I., 2015. Selecting crop models for decision making in wheat insurance. *European Journal of Agronomy*, 68, 97-116.
11. Ceglar, A., Toreti, A., Lecerf, R., Van der Velde, M. and Dentener, F., 2016. Impact of meteorological drivers on regional inter-annual crop yield variability in France. *Agricultural and Forest Meteorology*, 216, 58-67.
12. Confalonieri, R. and Bechini, L., 2004. A preliminary evaluation of the simulation model CropSyst for alfalfa. *European Journal of Agronomy*, 21(2), 223-237.
13. Confalonieri, R. and Bocchi, S., 2005. Evaluation of CropSyst for simulating the yield of flooded rice in northern Italy. *European Journal of Agronomy*, 23(4), 315-326.
14. DRDLR, 2013. Free State Province Spatial Development Framework (PSDF). Department of Rural Development and Land Reform. Pretoria.

15. Esfandiary, F., Aghaie, G. and Mehr, A.D., 2009. Wheat Yield Prediction through Agro Meteorological Indices for Ardebil District. *World Academy of Science, Engineering and Technology,* 49, 32-35.
16. Farré, I., Robertson, M.J., Walton, G.H. and Asseng, S., 2002. Simulating phenology and yield response of canola to sowing date in Western Australia using the APSIM model. *Crop and Pasture Science*, 53(10), 1155-1164.
17. Foody, G.M., 2003. Geographical weighting as a further refinement to regression modelling: an example focused on the NDVI–rainfall relationship. *Remote Sensing of Environment*, 88, 283–293.
18. Grenzdörffer, G.J., Engel, A. and Teichert, B., 2008. The photogrammetric potential of low-cost UAVs in forestry and agriculture. *The International Archives of the Photogrammetry, Remote Sensing and Spatial Information Sciences*, 31(B3), 1207-1214.
19. Hansen, P.M., Jørgensen, J.R. and Thomsen, A., 2002. Predicting grain yield and protein content in winter wheat and spring barley using repeated canopy reflectance measurements and partial least squares regression. *The Journal of Agricultural Science*, 139(03), 307-318.
20. Hoogenboom, G., 2000. Contribution of agrometeorology to the simulation of crop production and its applications. *Agricultural and forest meteorology*, 103(1), 137-157.
21. Ji, B., Sun, Y., Yang, S. and Wan, J., 2007. Artificial neural networks for rice yield prediction in mountainous regions. *The Journal of Agricultural Science*, 145(03), 249-261.
22. Jones, J.W., Hoogenboom, G., Porter, C.H., Boote, K.J., Batchelor, W.D., Hunt, L.A., Wilkens, P.W., Singh, U., Gijsman, A.J. and Ritchie, J.T. 2003. The DSSAT cropping system model. *European Journal of Agronomy*, 18(3), 235-265.
23. Kingra, P.K. and Prabhjyot-Kaur., 2013. Agroclimatic Study for Prediction of Growth and Yield of Brassica sp. in Central Punjab. *Journal of Agricultural Physics*, 13(2), 148-152.
24. Ko, J, Piccinni, G, Guo, W and Steglich, E., 2009. Parameterization of EPIC crop model for simulation of cotton growth in South Texas. *The Journal of Agricultural Science*, 147(02), 169-178.
25. Liu, J., 2009. A GIS-based tool for modelling large-scale crop-water relations. *Environmental Modelling & Software*, 24(3), 411-422.
26. Lobell, D.B., Ortiz-Monasterio, J.I., Asner, G.P., Matson, P.A., Naylor, R.L. and Falcon, W.P., 2005. Analysis of wheat yield and climatic trends in Mexico. *Field crops research*, 94(2), 250-256.
27. Lopresti, M.F., Di Bella, C.M. and Degioanni, A.J., 2015. Relationship between MODIS-NDVI data and wheat yield: A case study in Northern Buenos Aires province, Argentina. *Information Processing in Agriculture*, 2(2), 73-84.
28. Ma, B.L., Dwyer, L.M., Costa, C., Cober, E.R. and Morrison M.J., 2001. Early prediction of soybean yield from canopy reflectance measurements. *Agronomy Journal*, 93(6), 1227-1234.

29. Marcos, J., Cornet, D., Bussière, F. and Sierra, J., 2011. Water yam (Dioscorea alata L.) growth and yield as affected by the planting date: Experiment and modelling. *European Journal of Agronomy*, 34(4), 247-256.
30. Miglietta, F. and Bindi, M., 1993. Crop growth simulation models for Research, Farm Management and Agrometeorology. *Advances in Remote Sensing*, 2, 148-157.
31. Moussa, R., Chahinian, N. and Bocquillon, C., 2007. Distributed hydrological modelling of a Mediterranean mountainous catchment–Model construction and multi-site validation. *Journal of Hydrology*, 337(1), 35-51.
32. Mu, Q., Zhao, M. and Running, S.W., 2011. Improvements to a MODIS global terrestrial evapotranspiration algorithm. *Remote Sensing of Environment*, 115, 1781-1800.
33. NDA, 2005. Wheat. National Department of Agriculture. Pretoria.
34. Nonhebel, S., 1994. Inaccuracies in weather data and their effects on crop growth simulation results I. Potential production. *Climate Research*, 4, 61–74.
35. Oerke, E.C., 2006. Crop losses to pests. *The Journal of Agricultural Science*, 144, 31-43.
36. Palosuo, T., Kersebaum, K.C., Angulo, C., Hlavinka, P., Moriondo, M., Olesen, J.E., Patil, R.H., Ruget, F., Rumbaur, C., Takáç, J., Trnka, M., Bindi, M., Çaldağ, B., Ewert, F., Ferrise, R., Mirschel, W., Şaylan, L., Šiška, B. and Rötter, R., 2011. Simulation of winter wheat yield and its variability in different climates of Europe: A comparison of eight crop growth models. *European Journal of Agronomy*, 35, 103-114.
37. Pathak, H., Ladha, J.K., Aggarwal, P.K., Peng, S., Das, S., Singh, Y., Singh, B., Kamra, S.K., Mishra, B., Sastri, A.S.R.A.S., Aggarwal, H.P. and Gupta, R.K., 2003. Trends of climatic potential and on-farm yields of rice and wheat in the Indo-Gangetic Plains. *Field Crops Research*, 80, 223-234.
38. Prasad, A.K., Chai, L., Singh, R.P. and Kafatos, M., 2006. Crop yield estimation model for Iowa using remote sensing and surface parameters. *International Journal of Applied Earth Observation and Geoinformation*, 8(1), 26-33.
39. Ren, J., Chen, Z., Zhou, Q. and Tang, H., 2008. Regional yield estimation for winter wheat with MODIS-NDVI data in Shandong, China. *International Journal of Applied Earth Observation and Geoinformation*, 10(4), 403-413.
40. Rienecker, M.M., Suarez, M.J., Gelaro, R., Todling, R., Bacmeister, J., Liu, E., Bosilovich, M.G., Schubert, S.D., Takacs, L., Kim, G.K. and Bloom, S., 2011. MERRA: NASA's modern-era retrospective analysis for research and applications. *Journal of Climate*, 24(14), 3624-3648.
41. Rodell, M., Houser, P.R., Jambor, U.E.A., Gottschalck, J., Mitchell, K., Meng, J., Arsenault, K., Cosgrove, A., Radakovich, J., Bosilovich, M., Entin, J.K., Walker, J.P., Lohmann, D. and Toll, D., 2004. The global land data assimilation system. *Bulletin of the American Meteorological Society*, 85(3), 381-394.
42. Rosegrant, M.W. and Cline, S.A., 2003. Global food security: challenges and policies. *Science*, 302(5652), 1917-1919.

43. SAGL, 2013. South African Commercial Maize quality 2012/2013. South African Grain Laboratory. Pretoria.
44. Sun, J., 2000. Dynamic Monitoring and Yield Estimation of Crops by Mainly Using the Remote Sensing Technique in China. *Photogrammetric Engineering & Remote Sensing*, 66, 645-650.
45. Todorovic, M., Albrizio, R., Zivotic, L., Saab, M.T.A., Stöckle, C. and Steduto, P., 2009. Assessment of AquaCrop, CropSyst, and WOFOST models in the simulation of sunflower growth under different water regimes. *Agronomy Journal*, 101(3), 509-521.
46. Wendroth, O., Reuter, H.I. and Kersebaum, K.C., 2003. Predicting yield of barley across a landscape: a state-space modeling approach. *Journal of Hydrology*, 272(1), 250-263.

Chapter 5
Conclusion and Recommendations

5.1. Conclusion

This research was complementary to a bigger research programme aimed at understanding the application of satellite data and models to forecast grain yields and generate agricultural statistics for the summer rainfall regions of South Africa. The aim of the study was to assess the application of remotely sensed spectral indices derived from MODIS, and Landsat 8 with agrometeorological parameters to monitor dryland winter wheat health and forecast yields in the Free State Province. To guide this work, key research questions for the study were categorized into the following two groups:

a) The first group of questions concerned the broader issues of assessing and identifying;
    i. which indices were suitable for application in forecasting wheat yields and
    ii. whether the anthesis growth stage was relevant for use in developing yields models?
b) Group two dealt with assessing the influence of incorporating agrometeorological parameters in wheat yield forecasting models.

The research questions, main findings and limitations for each objective are summarized below:

Objective 1. To identify remotely sensed spectral indices that comprehensively describe wheat health status.

The research questions addressed in this objective were: can the LST (Land Surface Temperature) – vegetation index relationships be applied for wheat health status monitoring? Which spectral indices are best related to LST for wheat health status monitoring? The LST-vegetation index relationship has been applied mainly for studying Urban Heat Islands, land use change, and urban expansion (Jiang and Tian,

2010; Guo et al., 2012), in this objective, this relationship was applied for wheat health status monitoring. Moisture indices and vegetation abundance indices derived for Landsat 8 were evaluated against LST.

The LST was low at vegetated wheat farms, whereas, the Normalized Difference Vegetation Index (NDVI) and Green Normalized Difference Vegetation Index (GNDVI) were high at these wheat farms, the opposite trend was observed for fallow or harvested farms. The moisture indices were positively related to LST and wheat farms that were flourishing had a high moisture content. This observation is expected for wheat, the results demonstrated that healthy wheat releases more transpiration as compared unhealthy wheat (Kogan et al., 2005). The NDVI and Normalized Difference Water Index (NDWI) were suitable indices for monitoring the wheat health status as compared to the GNDVI and Normalized Difference Moisture Index (NDMI). A better fit was observed for the moisture indices as compared to the vegetation abundance indices.

The limitations of the study were that some of the Landsat 8 images were contaminated with cloud cover. Furthermore, because of crop rotations, some of the wheat farmers were not planting wheat at the same places consistently. This limited the samples and Landsat 8 images, which could be analyzed. Using the LST-vegetation index relationship, farmers can mitigate conditions hampering wheat growth such as a lack of moisture, fertilizer, pesticides or herbicides at stressed areas.

Objective 2. To develop a NDVI based wheat yield forecasting model.

The research questions addressed in this objective were: can the anthesis growth stage give accurate forecasts of yield? Can Moderate Resolution Imaging Spectroradiometer (MODIS) derived NDVI give accurate forecasts of wheat yield? The prospect of using MODIS-NDVI for winter wheat yield forecasts in the Central Free State production region was investigated using regression models. Findings suggest that the best time to relate MODIS-NDVI to final wheat yields for this area is the period leading to 30 days before harvest (first week of November). This period coincides with the anthesis stage, and at this time, wheat yield is highly correlated to NDVI. Aparicio

et al., (2002), Moriondo et al., (2007) and Lopresti et al., (2015) all determined that this stage was ideal for wheat yield estimations, forecasting wheat during this stage in Central Free State gave accurate forecasts of wheat yield.

The NDVI based linear regression model was accurate with an R^2 value of 0.73, a p-value of 0.00161 and an RMSE of 0.41 tons ha^{-1}. These results were similar to those observed by Lopresti et al., (2015) of an R^2 of 0.75 for winter wheat yield in Northern Buenos Aires province, Argentina. The similarities were because periods for winter wheat production are similar for both countries because the seasonal cycles coincide. However, Ren et al., (2008) observed an R^2 of 0.88 for Shandong (China) when relating the production of winter wheat with the accumulated MODIS derived NDVI. Becker-Reshef et al., (2010) reported an RMSE of 0.44 tons ha^{-1} and Moriondo et al., (2007) observed an RMSE of 0.44 tons ha^{-1} and 0.47 tons ha^{-1}, which are similar to those observed in this study. Diagnostic plots, model testing and validation provided evidence of the reasonable levels of model accuracy, model reliability, and a good fit.

The limitation of this study was that in some years, wheat farmers were not planting- this limitation was overcome by applying the threshold suggested by Ren et al., (2008) that NDVI values between 0.2 to 0.8 correspond to winter wheat. The evidence indicates that the use of MODIS data is reliable for wheat yield forecasting during the anthesis growth stage.

Objective 3. To evaluate the impact of agrometeorological parameters on the NDVI based wheat yield forecasting model.

The research questions addressed in this objective were: what is the impact of incorporating agrometeorological parameters to an NDVI based model? Which of the selected agrometeorological parameters are closely related to wheat yield? The NDVI was related to satellite derived soil moisture, evapotranspiration and surface temperature through a multi-linear regression model for wheat yield forecasting. The calibrated model explained 82% of the variability and a p-value of 0.0444 (<0.05) which meant that the model was statistically significant. These results were similar to those observed by Balaghi et al., (2008) of R^2 values of 0.64 to 0.98 for wheat grain yields

and Prasad et al., (2006) of R^2 values of 0.78 for maize and 0.86 for soybean. Model testing with independent data confirmed that the model had reasonable level of accuracy. Differences between the observed yield and the predicted yield were due to factors not accounted for in the model such as: pests, changes in planting date, weeds, and pathogens (Oerke, 2006; Pathak et al., 2003). The addition of agrometeorological parameters improved the NDVI based model from an R^2 of 0.73 to an R^2 of 0.82.

The parameters important for wheat yield modelling in the Central Free State were investigated using a correlation matrix. The NDVI (r=0.88) and evapotranspiration (r=0.58) were highly correlated to wheat yield compared to soil moisture (r=0.27) and land surface temperature (r=-0.02). These results were expected, as Moussa et al., (2007) determined that evapotranspiration is important for non-irrigated crops and there is evidence from prior studies that NDVI is related to crop yield, the same trend is observed for wheat in Central Free State (Benedetti and Rossini, 1993; Ma et al., 2001; Ren et al., 2008; Lopresti et al., 2015).

The limitation of this study was that in some years, wheat farmers were not planting, this limitation was overcome by applying the threshold suggested by Ren et al., (2008) that NDVI values between 0.2 to 0.8 correspond to winter wheat. This study demonstrated that remote sensing can be used for wheat yield modelling to overcome the problems of timeliness and cost of manual surveys for yield predictions in South Africa. The incorporation of agrometeorological parameters in the wheat yield model increased the predictive capacity of the yield models.

5.2. Recommendations

The recommendations based on the findings of this research are as follows:

- The study found that integrating agrometeorological parameters in wheat yield forecasting models improves their performance. Therefore, it is recommended that agrometeorological parameters should be integrated in wheat yield models to comprehensively describe the yield potential of an area when forecasting crop yield. The yield models should be updated annually where possible because they lose accuracy over time as the environmental conditions change.

- Cloud cover limited the Landsat 8 images analysed in the study during the process of evaluating spectral indices for wheat health status monitoring. Therefore, it is recommended that microwave sensors such as Synthetic Aperture Radar (SAR) should be considered for yield predictions because they operate on all weather conditions. Optical sensors are often not useful when cloud cover is present.

- Selected spectral indices were evaluated for wheat health in this research. However, different spectral indices from other satellite payloads such as the modified red edge NDVI (MRENDVI) and the Enhanced Vegetation Index (EVI) can be compared to the ones used in this study for wheat health status monitoring.

- This research made use of satellite derived agrometeorological data because the spatial distribution of weather stations was poor. However, data from ground stations e.g., weather stations can also be used if present where agricultural activity is prominent.

5.3. References

1. Aparicio, N., Villegas, D., Araus, J.L., Casadesus, J. and Royo, C., 2002. Relationship between growth traits and spectral vegetation indices in durum wheat. *Crop science*, 42(5), 1547-1555.
2. Balaghi, R., Tychon, B., Eerens, H. and Jlibene, M., 2008. Empirical regression models using NDVI, rainfall and temperature data for the early prediction of wheat grain yields in Morocco. *International Journal of Applied Earth Observation and Geoinformation*, 10(4), 438-452.
3. Becker-Reshef, I., Justice, C., Sullivan, M., Vermote, E., Tucker, C., Anyamba, A., Small, J., Pak, E., Masuoka, E., Schmaltz, J. and Hansen, M., 2010. Monitoring global croplands with coarse resolution earth observations: The Global Agriculture Monitoring (GLAM) project. *Remote Sensing*, 2(6), 1589-1609.
4. Benedetti, R. and Rossini, P., 1993. On the use of NDVI profiles as a tool for agricultural statistics: the case study of wheat yield estimate and forecast in Emilia Romagna. *Remote Sensing of Environment*, 45(3), 311-326.
5. Guo, Z., Wang, S.D., Cheng, M.M. and Shu, Y., 2012. Assessing the effect of different degrees of urbanization on land surface temperature using remote sensing images. *Procedia Environmental Sciences*, 13, 935-942.
6. Jiang, J. and Tian, G., 2010. Analysis of the impact of Land use/Land cover change on Land Surface Temperature with Remote Sensing. *Procedia Environmental Sciences*, 2, 571-575.
7. Kogan, F., Yang, B., Wei, G., Zhiyuan, P. and Xianfeng, J., 2005. Modelling corn production in China using AVHRR-based vegetation health indices*. International Journal of Remote Sensing*, 26(11), 2325-2336.
8. Lopresti, M.F., Di Bella, C.M. and Degioanni, A.J., 2015. Relationship between MODIS-NDVI data and wheat yield: A case study in Northern Buenos Aires province, Argentina. *Information Processing in Agriculture*, 2(2), 73-84.
9. Oerke, E.C., 2006. Crop losses to pests. *The Journal of Agricultural Science*, 144, 31-43.
10. Ma, B.L., Dwyer, L.M., Costa, C., Cober, E.R. and Morrison M.J., 2001. Early prediction of soybean yield from canopy reflectance measurements. *Agronomy Journal*, 93(6), 1227-1234.
11. Moriondo, M., Maselli, F. and Bindi, M., 2007. A simple model of regional wheat yield based on NDVI data. *European Journal of Agronomy*. 26, 266–274.
12. Moussa, R., Chahinian, N. and Bocquillon, C., 2007. Distributed hydrological modelling of a Mediterranean mountainous catchment–Model construction and multi-site validation. *Journal of Hydrology*, 337(1), 35-51.
13. Pathak, H., Ladha, J.K., Aggarwal, P.K., Peng, S., Das, S., Singh, Y., Singh, B., Kamra, S.K., Mishra, B., Sastri, A.S.R.A.S., Aggarwal, H.P. and Gupta, R.K., 2003. Trends of climatic potential and on-farm yields of rice and wheat in the Indo-Gangetic Plains. *Field Crops Research*, 80, 223-234.

14. Prasad, A.K., Chai, L., Singh, R.P. and Kafatos, M., 2006. Crop yield estimation model for Iowa using remote sensing and surface parameters. *International Journal of Applied Earth Observation and Geoinformation*, 8(1), 26-33.
15. Ren, J., Chen, Z., Zhou, Q. and Tang, H., 2008. Regional yield estimation for winter wheat with MODIS-NDVI data in Shandong, China. *International Journal of Applied Earth Observation and Geoinformation,* 10(4), 403-413.

Appendices

Appendix A1: The phenological growth of wheat

Wheat yields and quality are determined by a number of factors such as water availability (Asseng et al., 2002), changes in the planting date or climatic variables (i.e. temperature) and pests (Pathak et al., 2003). Water stress due to reduced rainfall is a dominant factor which causes decreased wheat yields (Dogan et al., 2007; Innes et al., 2015). Delays in the planting date of wheat causes late flowering, which forces the grain filling period to overlap with the high temperature regime, which affects the wheat quality (Singh et al., 2010). Additionally, high temperatures accelerate wheat development and decrease the grain filling period, which reduces wheat yields (Sharma, 1992; Sharma et al., 2008). Furthermore, pests such as weeds, pathogens and animals are responsible for 50% of the global potential loss of wheat (Oerke, 2006). The growth stages of wheat are described using the Feekes scale (Figure 15) which is outlined by Miller (1992) and Fageria et al., (1997).

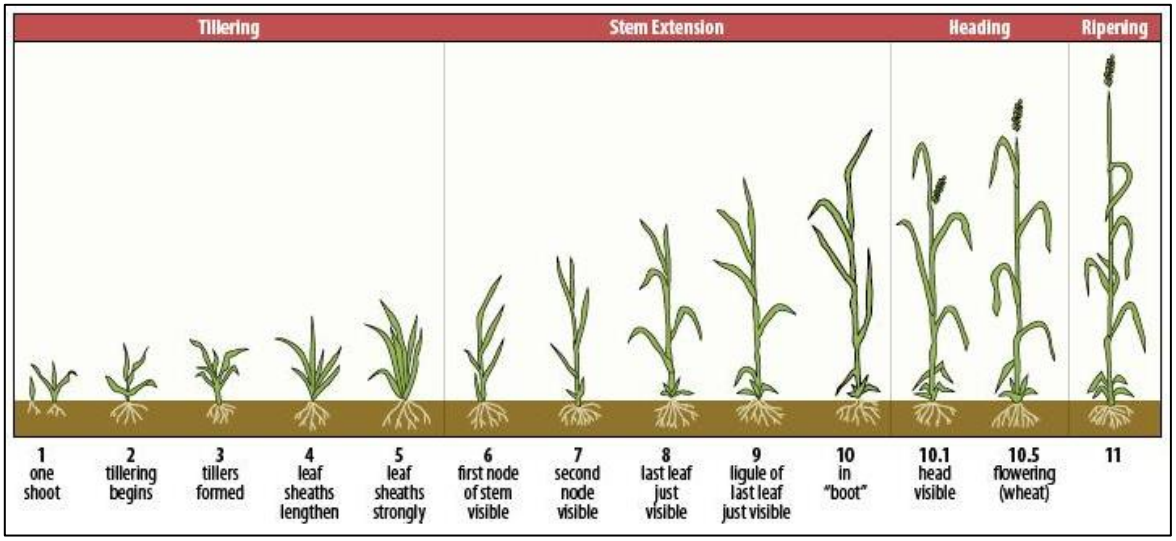

Figure 15. The growth stages of wheat according to the Feekes scale (Source: http://www.uky.edu/).

i. Feekes 1.0 - Seedling Emergence

The adapted seeds are planted in a fertile seedbed, which has enough moisture. It is important to plant the seeds at the right time as late planted wheat has less time to tiller and should be planted at high quantities to account for fewer tillers. At this stage, leaves are visible on the first shoot.

ii. Feekes 2.0 - Beginning of tillering

A tiller is a shoot, which emerges in the axil of a leaf (where the leaf joins the stem), or the coleoptile node (originates from the seed). The tillers have the same root mass as the original shoot or main stem. Once these tillers emerge, secondary tillers follow them from the axil of the primary tiller and the tertiary tillers develop from the axil of the secondary tillers and the process continues to form the tillers.

iii. Feekes 3.0 - Tillers formed

Winter wheat can tiller for many weeks. This process is dependent on factors such as the planting date and weather conditions. When there is winter dormancy, the process will be completed or disturbed. Measures should be taken to prevent weed infestation, which compete with the wheat for water, nutrients and light as a large number of tillers that are significant for grain yield are formed. At this stage, the leaves are twisted spirally.

iv. Feekes 4 .0 - Beginning of erect growth, leaf sheaths lengthen

The leaf sheaths continue elongating. Most of the tillers are formed prior to this stage and the secondary root system is starting to develop. The winter wheat begins to grow upright. Insect and weed control continues.

v. Feekes 5.0 - Leaf sheaths strongly erect

The tillers stop developing and the wheat grows vertically. Even wheat types, which grow horizontally or are low growing, start to grow upwards. This growth pattern is due to the leaf cover on the ground, which forms a false stem. The growth and size of

heads is determined. This takes place after vernalisation has completed, which causes the growing point below the soil at the crown to differentiate.

vi. Feekes 6.0 - 7.0- First node is visible followed by the second node

There is a change from vegetative growth to reproductive growth. The nodes are formed before this stage, but they are fused together and are not easy to visualize with the naked eye. The node gets swollen and is visible above the soil at Feekes stage 6. The head is above the node that gets pushed upwards, and the true stem starts to form, all the potential spikelets and florets are present. Then, the second node starts to appear above the soil next to the last leaf visible and the spike expands.

vii. Feekes 8.0 - 9.0 - Flag leaf is visible followed by the ligule of the flag leaf

The flag leaf starts to appear which is the last leaf. This leaf makes up 75% of the leaf area which contributes to grain fill. At this stage irrigation scheduling is important and the farmer can determine whether there are fungal disease on the wheat and whether there wheat is under stress. When the flag leaf has fully emerged at Feekes 9.0, army worms can cause significant damage to the yield potential.

viii. Feekes 10.0 –10.5 Boot stage and flowering

The first ears of wheat appear and the heading process proceeds until all the ears are out of the sheath. When the heading process is complete, flowering begins at the top and the base of the ear. The wheat undergoes self-pollination before the anthers come out.

ix. Feekes 11.0 - Ripening

The kernels of wheat go through the stages of milky ripening, when a milky fluid is present in the kernel, mealy ripening, when the kernel is starting to solidify and the kernels harden when the harvest is ready.

Appendix A2: The wheat growing calendar for Free State Province

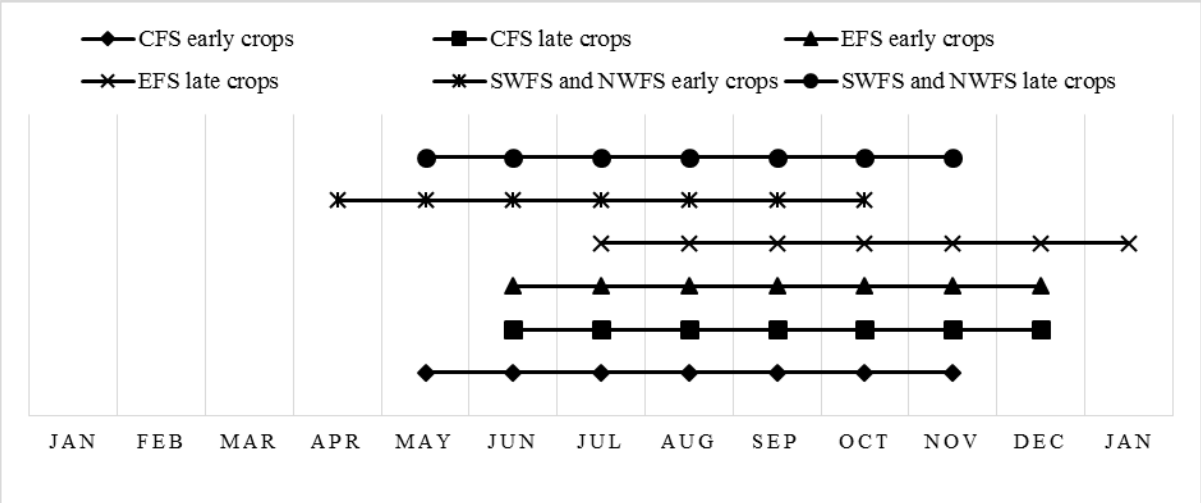

Figure 16. A schematic presentation of dryland wheat crop planting dates and duration in geographic regions of the summer rainfall area, (Free State) South Africa. SWFS - South Western Free State; NWFS - North Western Free State; CFS - Central Free State and EFS - Eastern Free State (Courtesy: Ernest Dube).

Appendix A3: Landsat 8 satellite characteristics

Table 7. Landsat 8 satellite bands (Source: http://landsat.usgs.gov).

Band number	Band	Wavelength (µm)	Resolution (m)
1	Coastal aerosol	0.43-0.45	30
2	Blue	0.45-0.51	30
3	Green	0.53-0.59	30
4	Red	0.64-0.67	30
5	Near Infrared	0.85-0.88	30
6	Short Wave Infrared (SWIR) 1	1.57-1.65	30
7	Short Wave Infrared (SWIR) 2	2.11-2.29	30
8	Panchromatic	0.50-0.68	15
9	Cirrus	1.36-1.38	30
10	Thermal Infrared (TIRS) 1	10.60-11.19	100 (resampled to 30m)
11	Thermal Infrared (TIRS) 2	11.50-12.51	100 (resampled to 30m)

Appendix A4: The Moderate Resolution Image Spectroradiometer technical specifications

Table 8. The Moderate Resolution Image Spectroradiometer characteristics (Source: http://modis.gsfc.nasa.gov).

Primary Use	Band	Bandwidth (μm)	Spectral Radiance ($W/m^2.\mu m.sr$)	SNR*	Spatial Resolution at Nadir (m)
Land/cloud	1	0.620-0.670	21.8	128	250
Boundaries	2	0.841-0.876	24.7	201	
Land/cloud	3	0.459-0.479	35.3	243	500
Properties	4	0.545-0.565	29.0	228	
	5	1.230-1.250	5.4	74	
	6	1.628-1.652	7.3	275	
	7	2.105-2.155	1.0	110	
Ocean colour/	8	0.405-0.420	44.9	880	1000
phytoplankton/	9	0.438-0.448	41.9	838	
biogechemistry	10	0.483-0.493	32.1	802	
	11	0.526-0.536	27.9	754	
	12	0.546-0.556	21.0	750	
	13	0.662-0.672	9.5	910	
	14	0.673-0.683	8.7	1087	
	15	0.743-0.753	10.2	586	
	16	0.862-0.877	6.2	516	
Atmospheric water	17	0.890-0.920	10.0	167	1000
vapour	18	0.931-0.941	3.6	57	
	19	0.915-0.965	15.0	250	

*Signal-to-noise ratio

Table 8. continued

Primary Use	Band	Bandwidth (μm)	Spectral Radiance ($W/m^2.\mu m.sr$)	Required NEΔT* (K)	Spatial Resolution at Nadir (m)
Surface/cloud temperature	20	3.660-3.840	0.45	0.05	1000
	21	3.929-3.989	2.38	2.00	
	22	3.929-3.989	0.67	0.07	
	23	4.020-4.080	0.79	0.07	
Atmospheric Temperature	24	4.433-4.498	0.17	0.25	1000
	25	4.482-4.549	0.59	0.25	
Cirrus clouds	26	1.360-1.390	6.00	150 (SNR)	1000
	27	6.535-6.895	1.16	0.25	
	28	7.175-7.475	2.18	0.25	
	29	8.400-8.700	9.58	0.05	
Ozone	30	9.580-9.880	3.69	0.25	1000
Surface/cloud Temperature	31	10.780-11.280	9.55	0.05	1000
	32	11.770-12.270	8.94	0.05	
Cloud Top Altitude	33	13.185-13.485	4.52	0.25	1000
	34	13.485-13.785	3.76	0.25	
	35	13.785-14.085	3.11	0.25	
	36	14.085-14.385	2.08	0.35	

*Noise-equivalent temperature difference

Appendix A5: The Moderate Resolution Image Spectroradiometer tiles for Central Free State

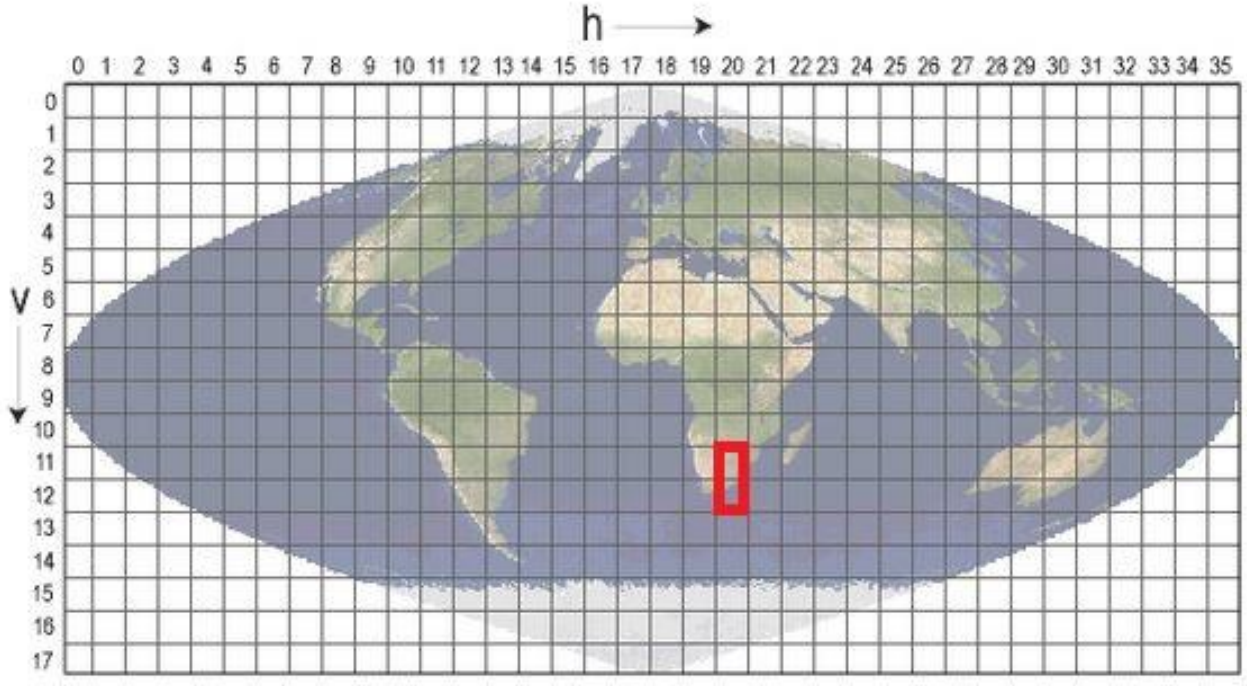

Figure 17. The MODIS tiles for Central Free State in Sinusoidal projection (Source: http://modis-land.gsfc.nasa.gov).

Appendix A6: Parameters for the yield models

Table 9. The parameters used for developing the NDVI and agrometeorological parameter based models.

Years	Yield	NDVI	SM	ET	ST
2000	2.8971	0.4115	0.2764	32.7896	22.8568
2001	2.7700	0.4419	0.1866	47.8624	24.2016
2002	1.9900	0.3685	0.1593	14.4091	23.1671
2003	1.0742	0.3141	0.1868	17.4989	25.2286
2004	1.2697	0.3403	0.1556	12.0075	24.9303
2005	1.1170	0.3628	0.1918	22.5237	25.4442
2006	2.7885	0.4372	0.1774	33.1656	26.1245
2007	2.8459	0.4290	0.1922	30.4485	25.3217
2008	1.2400	0.3055	0.2132	27.2331	25.6317
2009	2.7575	0.4872	0.1920	31.3410	25.8742
2010	2.3952	0.4125	0.1875	20.0611	26.1694
2011	1.7100	0.3667	0.1694	12.8948	25.0812
2012	2.2734	0.4527	0.1713	21.3315	25.8417
2013	2.6513	0.4290	0.1773	17.2055	26.4126
2014	2.4000	0.4307	0.1974	22.8780	26.1047

References

1. Asseng, S., Turner, N.C., Ray, J.D. and Keating, B.A., 2002. A simulation analysis that predicts the influence of physiological traits on the potential yield of wheat. *European Journal of Agronomy*, 17, 123-141.
2. Dogan, E., Kirnak, H. and Copur, O., 2007. Effect of seasonal water stress on soybean and site specific evaluation of CROPGRO-Soybean model under semi-arid climatic conditions. *Agricultural Water Management*, 90, 56-62.
3. Fageria, N.K., Baligar, V.C. and Jones, C.A., 1997. *Growth and Mineral Nutrition of Field Crops*. 3rd Ed. CRC Press. Virgin Islands.
4. Innes, P.J., Tan, D.K.Y., Van Ogtrop, F. and Amthor, J.S., 2015. Effects of high-temperature episodes on wheat yields in New South Wales, Australia. *Agricultural and Forest Meteorology*, 208, 95-107.
5. Miller, T.D., 1992. Growth Stages of Wheat: Identification and Understanding Improve Crop Management. *Better Crops with Plant Food*. 76, 12-17.
6. Oerke, EC, 2006. Crop losses to pests. *The Journal of Agricultural Science*, 144, 31-43.
7. Pathak, H., Ladha, J.K., Aggarwal, P.K., Peng, S., Das, S., Singh, Y., Singh, B., Kamra, S.K., Mishra, B., Sastri, A.S.R.A.S., Aggarwal, H.P. and Gupta, R.K., 2003. Trends of climatic potential and on-farm yields of rice and wheat in the Indo-Gangetic Plains. *Field Crops Research*, 80, 223-234.
8. Sharma, R.C., 1992. Duration of the vegetative and reproductive period in relation to yield performance of spring wheat. *European Journal of Agronomy*, 1, 133-137.
9. Sharma, R.C., Tiwary, A.K. and Ortiz-Ferrara, G., 2008. Reduction in kernel weight as a potential indirect selection criterion for wheat grain yield under terminal heat stress. *Plant breeding*, 127, 241-248.
10. Singh, S., Gupta, A.K., Gupta, S.K., and Kaur, N., 2010. Effect of sowing time on protein quality and starch pasting characteristics in wheat (Triticum aestivum L.) genotypes grown under irrigated and rain-fed conditions. *Food Chemistry*, 122, 559-565.